ACCSCIENCE PUBLISHING

International Journal of Bioprinting

REVIEW ARTICLE

Synergistic 3D bioprinting and electrical stimulation for advanced electroactive tissue regeneration

Jinwei Huang, Jiaming Wu, Jinglin Ye, Lihu Chen, Wenxiao Fang, and Huachun Wang*

School of Integrated Circuits, Shenzhen Campus of Sun Yat-sen University, Shenzhen, Guangdong, China

Abstract

Severe tissue injuries often disrupt the body's endogenous electric fields, making spontaneous healing nearly impossible. Although exogenous electrical stimulation (ES) is an effective intervention, conventional rigid electrodes are mechanically and geometrically incompatible with soft, dynamic biological tissues. To address this problem, three-dimensional (3D) bioprinting with conductive bioinks has emerged as a transformative strategy to create biomimetic, electroactive scaffolds. This review explores how combining 3D-printed scaffolds with ES promotes complex tissue regeneration. We first analyze the core cellular mechanisms by which ES accelerates tissue repair (e.g., guiding cell migration, enhancing proliferation, and directing differentiation). We then summarize the mainstream 3D printing techniques (extrusion-based, inkjet, laser-assisted, photocuring-based printing) and detail the development of conductive bioinks from basic polymers to advanced electroactive materials, including piezoelectric, triboelectric, magnetoelectric, bio-battery, and optoelectronic materials for wireless stimulation. This synergistic strategy has been widely used to repair various tissue defects, including skin, nerve, bone, muscle, and cardiac tissue injuries, and shows considerable therapeutic promise. Finally, we discuss ongoing clinical hurdles and offer a practical roadmap toward programmable scaffolds and closed-loop systems. Overall, this field is rapidly shifting from passive structural support to active electrophysiological guidance, laying the foundation for next-generation smart tissues.

Keywords: 3D bioprinting; Electrical stimulation; Conductive bioinks; Electroactive scaffolds; Tissue regeneration; Bioelectronics

***Corresponding author:**
Huachun Wang
(wanghch36@mail.sysu.edu.cn)

Citation: Huang J, Wu J, Ye J, Chen L, Fang W, Wang H. Synergistic 3D bioprinting and electrical stimulation for advanced electroactive tissue regeneration. *Int J Bioprint.* 2026;12(4):026220216. doi: 10.36922/IJB026220216

Received: May 26, 2026

Revised: June 25, 2026

Accepted: June 30, 2026

Published online: June 30, 2026

1. Introduction

Endogenous electric fields (EFs) generated by cells, tissues, and organs during physiological processes play a crucial role in maintaining homeostasis by modulating cellular behaviors.[1,2] Under normal conditions, injury-induced EFs act as vital cues, guiding cell behavior toward regeneration.[3,4] However, in severe pathological states such as volumetric defects, complete nerve transections, or chronic diabetic ulcers, the native EFs at the lesion site are often irreversibly disrupted, rendering spontaneous regeneration via self-regulation ineffective. Consequently, exogenous electrical stimulation (ES)

has been developed to artificially reconstruct these lost electrophysiological gradients.[5-7] Although conventional electroceuticals have shown potential for accelerating tissue repair, their clinical translation remains constrained by the physicochemical incompatibility between rigid, planar electronic devices and soft, irregularly shaped biological tissues. This mismatch causes inefficient signal transmission, limited conformal contact, and potentially mechanical damage.[8] Therefore, a key challenge in tissue engineering is to construct a physical scaffold that can seamlessly integrate with native tissue architecture and perform as a functional interface for exogenous ES.

Three-dimensional (3D) bioprinting has emerged as a powerful tool to address this structural challenge. Through the precise, layer-by-layer deposition of bioinks, extrusion-, inkjet-, laser-assisted, and photocuring-based printing technologies can replicate the multiscale structural features of native extracellular matrix (ECM), ranging from macroscopic geometry down to microscale porosity.[9,10] This capability effectively overcomes the mechanical mismatch between conventional rigid devices and soft tissues.[11] However, most 3D-printed bioscaffolds made of non-conductive polymers (e.g., gelatin, polylactic acid) are electrically inert and incapable of conducting or mediating exogenous ES.[12-14] Therefore, successfully combining 3D printing and ES depends on developing electrically active bioinks that provide both structural biomimicry and effective signal transmission.

The evolution of such conductive bioinks has gone through several stages. Early efforts using intrinsic conductive polymers (e.g., polypyrrole [PPy], polyaniline [PANI]) were limited by poor processability and biocompatibility.[15] Subsequently, conductive nanomaterials (e.g., carbon nanotubes [CNTs], metal nanoparticles) were embedded into biocompatible matrices to balance conductivity and cytocompatibility.[16,17] Further blending with natural or synthetic polymers yielded composite scaffolds capable of both efficient electrical signal transmission and ECM-mimetic niche support.[18,19] More recently, research focus has shifted from static conductive frameworks to wireless electroactive scaffolds based on self-powered piezoelectric and triboelectric effects, and has further extended to magnetoelectric, biobattery, and optoelectronic systems.[20-22] These advanced materials harvest ambient energy (e.g., mechanical, magnetic, biochemical, or light) and convert it into localized EFs, enabling on-demand ES without implanted electrodes or external power sources. This synergistic strategy of 3D-printed electroactive bioscaffolds that conduct exogenous ES or generate localized electrical cues can overcome the limits of insulating scaffolds and/or rigid electrotherapy devices, greatly boosting the potential for clinical translation.

In this review, we explore the state-of-the-art advances in the synergistic application of 3D-printed electroactive scaffolds and exogenous ES for tissue regeneration. We first summarize five key mechanisms by which ES promotes regenerative processes at molecular and cellular levels: guiding migration, enhancing proliferation, directing differentiation, regulating apoptosis, and promoting growth factor secretion. We then analyze the technological characteristics of four mainstream 3D printing modalities (inkjet, extrusion-based, laser-assisted, and photocuring-based) and review the development of conductive bioink design, from early conductive polymers and nanoparticle-doped composites to emerging electroactive materials. Next, we highlight recent applications of this synergistic approach in wound healing, as well as in the repair of nerve, bone, muscle, and cardiac defects (Figure 1). Finally, we discuss current challenges, such as long-term biocompatibility, degradation kinetics matching, and ES protocol standardization, and offer a roadmap for these technologies from the lab to clinical use.

2. Mechanisms by which electrical stimulation promotes tissue repair

Bioelectricity is a crucial factor in maintaining physiological homeostasis, ensuring the normal functioning of various organs through cellular regulation.[1] As a biophysical intervention, non-invasive ES has demonstrated considerable potential in tissue repair. By mimicking endogenous bioelectricity, it regulates a range of cellular behaviors, including migration, proliferation, differentiation, apoptosis, modulation of the inflammatory microenvironment, and secretion of growth factors,[8,23,24] thereby accelerating the tissue repair and remodeling processes. When combined with 3D-printed conductive and electroactive scaffolds, ES synergistically promotes tissue repair through five primary mechanisms (Figure 2).

2.1. Cell migration

Electrotaxis refers to the directed migration of cells under an EF and is a fundamental process in wound healing and endogenous tissue regeneration. Although the precise mechanisms driving this migration remain incompletely understood, studies indicate that it is governed by multiple factors. For instance, ES can activate specific receptors on the cell membrane (such as the epidermal growth factor receptor, acetylcholine receptors, and integrins), thereby triggering downstream signal transduction cascades. Among these, MAPK-ERK1/2 and PI3K/Akt serve as the two core signaling pathways regulating electrotaxis.[25,26]

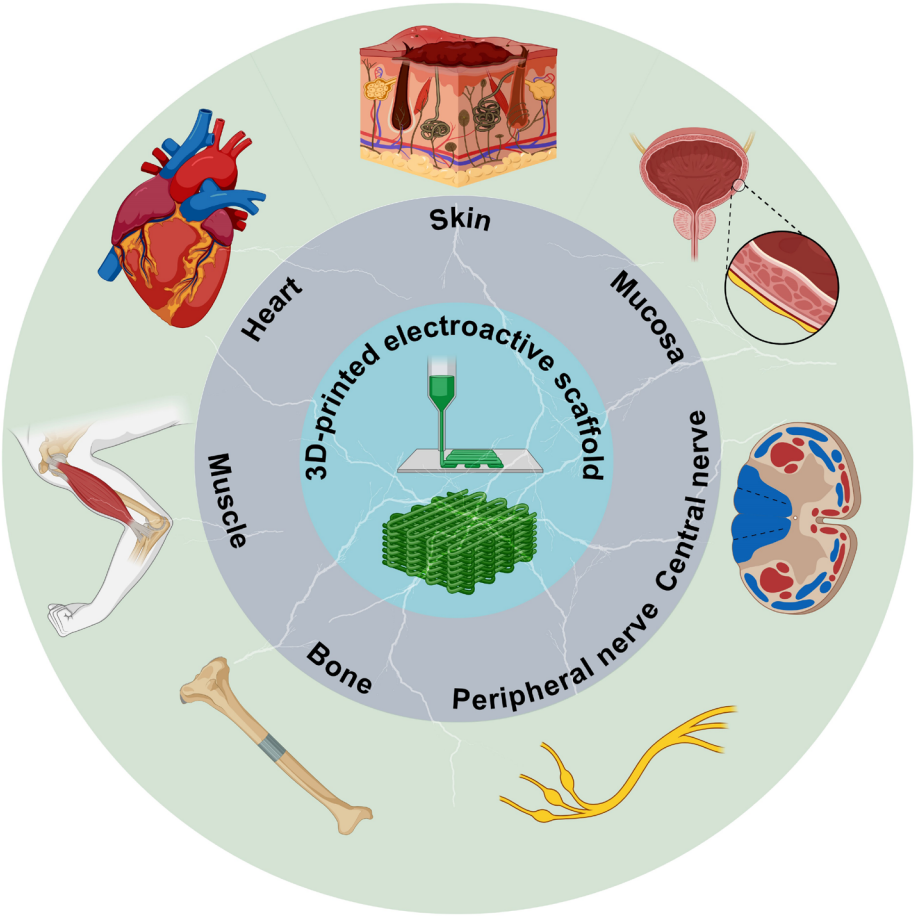

Figure 1. Schematic illustration of the holistic strategy combining 3D bioprinting and electrical stimulation for multi-tissue defect repair. Created in BioRender. Huang, J. (2026) https://BioRender.com/81amucy.

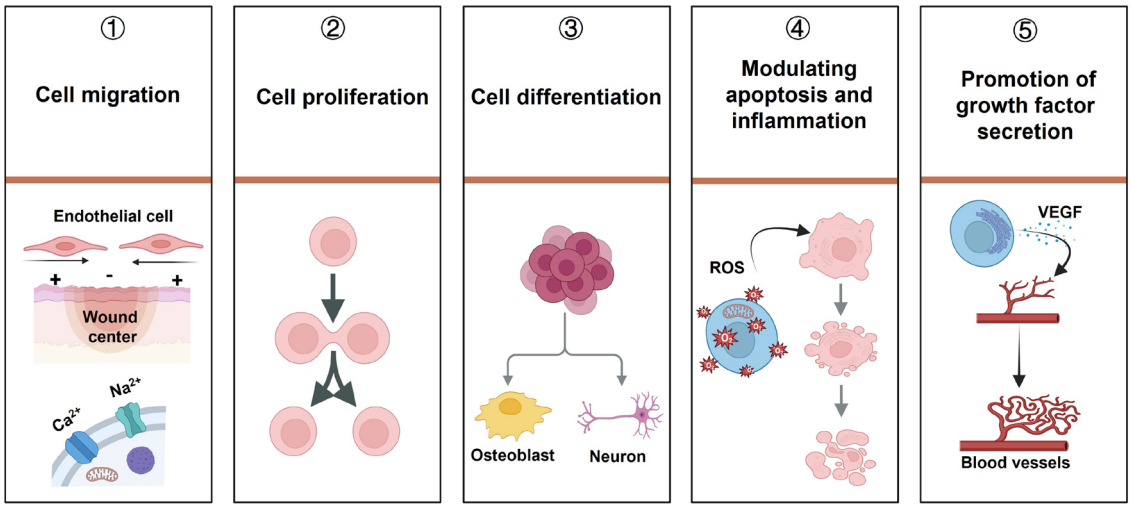

Figure 2. Schematic illustration of the biophysical and cellular mechanisms underlying electrical stimulation-mediated tissue regeneration. Created in BioRender. Huang, J. (2026) https://BioRender.com/u0arb3o.
Abbreviations: ROS: Reactive oxygen species; VEGF: Vascular endothelial growth factor.

EFs can induce the asymmetrical distribution of epidermal growth factor receptor at the cell poles,[27] activating PI3K to cause the accumulation of PIP3 on the membrane, which directs the rearrangement of cytoskeletal proteins and ultimately leads to directional cell migration. In addition to signaling pathways, EFs can also activate voltage-gated calcium (Ca^{2+}) and sodium (Na^{+}) channels, increasing cellular ion influx to further modulate cytoskeletal polarization and motility.[28,29]

2.2. Cell proliferation

Researchers have demonstrated that ES can promote the proliferation of various cell types, including fibroblasts, myocytes, and hair follicle cells, among others.[8] EFs exert regulatory effects on multiple stages of the cell cycle, primarily involving gene transcription and translation. At the transcriptional level, EFs can modulate gene expression via pathways such as nuclear factor-kappa B, thereby accelerating cell proliferation.[30,31] At the translational level, ES modulates the activity of specific metabolic enzymes, thereby enhancing ribosome-mediated protein synthesis and expediting cell proliferation.[32] Furthermore, low-intensity ES enhances cellular proliferation by increasing *PCNA* expression and stimulating signaling pathways involved in cell cycle progression.[24]

2.3. Cell differentiation

In tissue engineering, ES can direct stem cell differentiation via complex intracellular signal transduction, the redistribution of cell membrane receptors, and alterations in transmembrane potentials.[33] EF-induced membrane depolarization triggers the opening of voltage-gated Ca^{2+} channels, leading to intracellular Ca^{2+} influx and subsequent regulation of Ca^{2+} signaling and energy metabolism between the endoplasmic reticulum and mitochondria. These events activate the Ca^{2+}/calmodulin-dependent protein kinase II pathway, a key regulator of cell fate determination and lineage-specific differentiation.[34,35] Studies have demonstrated that ES with specific parameters can upregulate the expression of osteogenesis-related genes (e.g., type I collagen, type II collagen, and Runx2) and enhance Ca^{2+} deposition within the ECM, thereby inducing the osteogenic differentiation of bone marrow mesenchymal stem cells (BMSCs).[36] Similarly, ES can promote the differentiation of neural stem cells (NSCs) into functional neurons and facilitate neurite outgrowth.[33]

2.4. Regulation of apoptosis and the inflammatory environment

Electrical stimulation exhibits a dual regulatory capacity for maintaining microenvironmental homeostasis and clearing abnormal tissues. In the early stages of tissue repair, EFs can alter cell membrane permeability, leading to Ca^{2+} influx and inducing the generation of reactive oxygen species within mitochondria. This process influences Bcl-2 family proteins (which regulate the balance between pro- and anti-apoptotic proteins) or modulates death receptor pathways on the cell membrane, thereby facilitating the clearance of inflammatory cells.[37,38] This helps to mitigate excessive inflammatory responses in tissues, establishing a favorable condition for subsequent healing. Conversely, in electro-sensitive tissues such as nerves and muscles, ES can activate the PI3K–Akt signaling pathway, exerting pronounced anti-apoptotic and cytoprotective effects.[25] Furthermore, specific patterns of EFs can drive the polarized rearrangement of pro-repair receptors on macrophage membranes while activating Ca^{2+} influx mediated by channels such as TRPM7. This directs the polarization of macrophages toward the M2 phenotype (a pro-tissue repair and vascularization phenotype), accelerating the transition of the tissue from the inflammatory phase to the proliferative phase.[39] In the later stages of inflammation, ES can also downregulate the expression of pro-inflammatory cytokines, such as interleukin-6 and tumor necrosis factor, and reduce the number of mast cells, thereby accelerating the resolution of inflammation and preventing wound chronicity.[40]

2.5. Promotion of growth factor secretion

Electrical stimulation can optimize intracellular energy metabolism (increasing ATP production), trigger endoplasmic reticulum stress responses, and induce the reorganization of Golgi structures, thereby enhancing cellular protein synthesis and exocytotic secretion.[34,41,42] In response to exogenous EFs, the nitric oxide synthase pathway is activated, stimulating local cells to upregulate the secretion of key molecules such as vascular endothelial growth factor (VEGF), fibroblast growth factors (FGF-1, FGF-2), insulin-like growth factor, and brain-derived neurotrophic factor. The elevated level of angiogenic factors upregulates the expression of CXCR4 and CXCR2 receptors on the surface of endothelial cells, facilitating the assembly of nascent capillary networks that supply sufficient oxygen and nutrients to the defect region. Concurrently, the secretion of neurotrophic factors induces reinnervation within the damaged tissue, ensuring the survival and functional recovery of the regenerated tissue.[23,27,43,44]

Elucidating this pathway from physical signals to cellular responses and tissue remodeling marks a fundamental shift in tissue engineering. It moves from passive structural bridging to active electrophysiological orchestration. Yet most current studies treat ES as a static or uniform input, overlooking the dynamic nature of

endogenous EFs during regeneration. The real challenge ahead is not simply building better conductive scaffolds, but creating intelligent systems that can adapt their electrical cues in space and time. Achieving this precise spatiotemporal matching will be key to translating smart bioelectronic scaffolds into clinical reality.

3. 3D bioprinting technologies

As a core cutting-edge technology in tissue engineering, 3D bioprinting offers a solution for fabricating functional tissue constructs to replace damaged or diseased tissues. This technology enables the high-precision and highly reproducible construction of complex 3D spatial structures, demonstrating significant potential for scalable production. To date, a multitude of 3D bioprinting technologies have been developed, each possessing distinct advantages and specific applications. However, the most extensively utilized and broadly applicable printing modalities primarily consist of four main categories: extrusion-based, inkjet-based, laser-assisted, and photocuring-based printing, as shown in **Figure 3**.

3.1. Extrusion-based printing

Extrusion-based bioprinting is currently the most widely utilized and established technology in tissue engineering. Its fundamental principle relies on pneumatic or mechanical driving forces, which can be broadly categorized into pneumatic, piston-driven, and screw-driven systems, as shown in Figure 3a. These mechanisms operate by extruding highly viscous bioinks from a syringe cartridge through a nozzle as continuous filaments. Subsequently, these filaments are deposited and solidified layer-by-layer along pre-designed 3D pathways.

In the construction of conductive scaffolds, extrusion-based bioprinting exhibits distinct advantages. Beyond its simple manufacturing technique, cost-effectiveness, and operational flexibility, it possesses the distinct capability to print bioinks characterized by high viscosity and non-Newtonian fluid behavior (accommodating viscosities up to 6×10^7 mPa·s).[45] This makes it highly suited for processing high-solid-content hydrogel systems that incorporate high concentrations of conductive fillers (e.g., CNTs, graphene) or high-molecular-weight conductive polymers.[46] The incorporation of such high-concentration fillers is imperative for establishing interconnected conductive networks within the scaffolds, thereby ensuring the efficient transduction of electrical signals.

Nevertheless, conventional extrusion-based bioprinting faces inherent challenges in processing conductive bioinks. High concentrations of conductive nanofillers and heterogeneous hydrogel formulations are prone to aggregation within the narrow nozzle lumen, often resulting in nozzle clogging. This consequently induces flow rate fluctuations and non-uniform material deposition. Second, the printing resolution of this technique is relatively low (typically >100 μm),[47] rendering it inadequate for the fabrication of high-precision 3D architectures. Furthermore, the intense shear and extensional stresses generated during the forced extrusion of highly viscous bioinks can inflict substantial mechanical damage on the encapsulated cells. Under this printing modality, cell viability typically ranges from 40% to 80%, with higher extrusion pressures consistently resulting in diminished cell survival rates.[48]

3.2. Inkjet-based printing

Inkjet bioprinting is a non-contact additive manufacturing technique based on microdroplet deposition. Depending on the physical mechanisms of droplet generation, this technology is primarily classified into continuous inkjet and drop-on-demand (DOD) inkjet. Continuous inkjet has not been widely adopted in bioprinting, mainly due to its instability and high susceptibility to contamination. In contrast, DOD technology has found extensive applications in biomedicine and tissue engineering. Based on its core actuation mechanisms, DOD inkjet is further subdivided into thermal and piezoelectric modalities (as shown in Figure 3b): thermal inkjet employs micro-resistors to rapidly heat the fluid within microseconds, generating vapor bubbles whose expansive pressure forcefully ejects the droplets; piezoelectric inkjet utilizes the mechanical deformation of piezoelectric ceramic elements driven by alternating electrical signals to generate instantaneous compressive stress. Both inkjet modalities are capable of ejecting low-viscosity bioinks at high speeds and micrometer-level precision onto a receiving substrate, where they subsequently spread, crosslink, and solidify.[45,49]

In addition to its low manufacturing costs and high operational efficiency, inkjet bioprinting provides excellent deposition precision and spatial resolution for electroactive scaffold construction. The technique allows patterned deposition of conductive bioinks onto substrates, using nozzle diameters as small as 18 μm.[50] Furthermore, piezoelectric inkjet printing can achieve high cell viability (>85%) and even possesses the ultra-high precision requisite to encapsulate a single cell within an individual microdroplet.[49]

However, inkjet printing is subject to stringent fluidic and rheological constraints when processing conductive bioinks. First, this technique imposes rigorous demands on the surface tension and viscosity of the bioinks, typically requiring a viscosity range of 1–25 mPa·s.[51]

Furthermore, when incorporating high concentrations of conductive nanofillers or high-density cell suspensions into low-viscosity bioinks, these suspended particles are highly susceptible to gravity-induced rapid sedimentation and microscopic agglomeration. Such irreversible agglomeration leads to severe nozzle clogging, thereby disrupting the continuity of the printing process and the uniformity of material deposition. Additionally, the localized heating inherent to thermal inkjet printing (typically reaching 200–300 °C), combined with the impact velocity of the droplets and subsequent material accumulation, can further compromise overall cell viability.[52,53]

3.3. Laser-assisted printing

Laser-assisted bioprinting is a high-precision, nozzle-free, and non-contact printing technology that utilizes high-energy laser pulses to drive material transfer. A typical setup comprises a focused laser beam, a donor ribbon coated with a light-absorbing sacrificial layer and the bioink, and a receiving substrate. Upon irradiation of the sacrificial layer by the laser pulse, localized and instantaneous vaporization occurs, generating a high-pressure vapor bubble, and the expansion of this bubble propels the bioink away from the donor film, as shown in Figure 3c.[54,55]

In the realm of electroactive tissue engineering, laser-assisted printing demonstrates three distinct advantages. First, its unique nozzle-free mechanism bypasses conventional rheological constraints, eliminating the clogging issues typically caused by conductive fillers. Second, the room-temperature working environment and zero-shear technology not only prevent shear damage during the extrusion process, but the ultra-short femtosecond pulses also enable printing with virtually no heat transfer, which preserves high cell viability in biological cell printing applications. Furthermore, this technology exhibits outstanding control over 3D spatial positioning and structural dimensions.[50,55,56] Recent studies have demonstrated that near-infrared laser-assisted printing can deposit ultra-fine microdroplets with diameters as small as 58 μm, reaching an ultimate resolution capable of

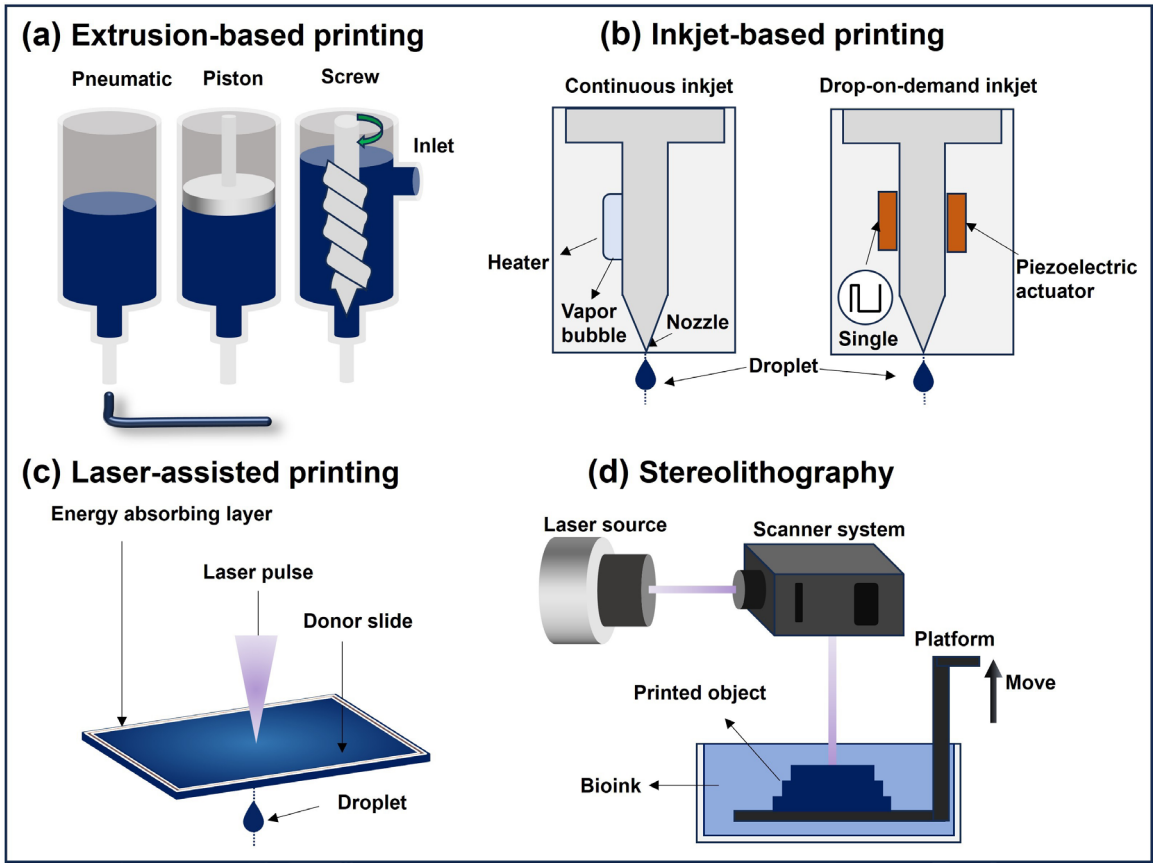

Figure 3. Schematic illustration of the four mainstream 3D bioprinting technologies. (a) Extrusion-based printing. (b) Inkjet printing. (c) Laser-assisted printing. (d) Stereolithography. Figure created by the authors using Microsoft PowerPoint.

encapsulating one to three cells per droplet. This capability holds significant clinical translational value for the construction of complex biological tissue models.[57]

Despite its advantages, this technology remains constrained by several challenges, including the high cost of laser systems, complex donor-layer fabrication, and the difficulty of constructing mechanically robust 3D architectures along the Z-axis. These limitations have restricted its scalability and clinical translation in electroactive tissue repair.

3.4. Photocuring-based printing

Photocuring-based bioprinting represents a class of vat photopolymerization technologies driven by photo-initiated chemical crosslinking reactions. Its primary modalities include stereolithography (SLA), digital light processing (DLP), and two-photon polymerization (2PP). Distinct from extrusion-dependent physical processes, this technique utilizes specific wavelengths of light to irradiate liquid photosensitive bioinks containing photoinitiators. This triggers an instantaneous polymerization reaction under the light field, enabling layer-by-layer or continuous curing and shaping.[58]

Although these three technologies are all based on the principle of photopolymerization, they exhibit significant differences in their light modulation methods and fabrication characteristics. SLA employs a single tightly focused laser beam to perform point-by-point scanning crosslinking on the liquid surface. While it yields extremely smooth fabricated surfaces, its printing speed is limited by the cross-sectional area. DLP, on the other hand, utilizes a digital micromirror device to project a single-layer sliced image onto the liquid surface simultaneously, achieving instantaneous whole-layer curing via surface exposure. This area-independent, ultra-high fabrication efficiency significantly reduces the *in vitro* printing time for cells, making it highly favored for live-cell processing. In contrast, 2PP utilizes femtosecond lasers to induce non-linear optical effects, wherein polymerization only occurs at the focal point where photon energy is intensely concentrated. This unique mechanism allows it to surpass the traditional optical diffraction limit, enabling ultra-high-resolution printing at the sub-micron or even nanoscale level.[59-61]

In tissue repair strategies combining ES, photocuring technologies possess unique advantages. They offer extremely high spatial resolution, capable of printing highly complex internal microstructures and anisotropic topographical morphologies with high fidelity. Notably, 2PP has achieved a resolution as low as approximately 100 nm.[62] Such precise microgrooves or oriented porous structures play a crucial role in guiding the directional extension of nerve axons and the polarized fusion of skeletal muscle cells. Simultaneously, the static crosslinking nature within the resin vat achieves an inherent zero-shear-stress condition, providing an optimal survival environment for fragile cells.[63,64]

Nevertheless, when applied to electroactive materials, this technology faces a significant challenge of optical shielding. Since the vast majority of highly conductive nanofillers are dark and opaque, they induce strong light scattering and absorption within the bioink. This leads to a precipitous drop in the light penetration depth, subsequently causing incomplete local curing or a loss of interlayer adhesion.[65] Therefore, balancing the optical transmittance of photosensitive bioinks with the density of the conductive network remains the core technical barrier currently facing photocuring-based conductive bioprinting.[66]

3.5. Emerging trends in 3D bioprinting technologies

Although the mainstream 3D bioprinting technologies discussed above have laid a solid foundation for electroactive tissue engineering, individual printing modalities often encounter specific limitations in practical applications. It is challenging to simultaneously balance high printing resolution, high cell viability, and the stringent rheological requirements for processing complex conductive bioinks. To overcome these inherent limitations, current bioprinting technologies are undergoing a profound iterative evolution, transitioning from singular to hybrid systems and from macroscopic to micro/nanoscale dimensions.

Regarding the in-depth advancement of individual technologies, conventional extrusion-based printing has evolved to encompass advanced processes such as coaxial extrusion, microfluidic-assisted extrusion, and cryobioprinting. Coaxial extrusion, through the instantaneous fluidic shaping of core-shell structures, offers an optimal strategy for constructing biomimetic nerve guidance conduits (NGCs) and hollow vascular networks.[67,68] Microfluidic-assisted nozzles enable the microscale *in situ* rapid mixing of crosslinkers and conductive precursors, which substantially mitigates the agglomeration and clogging issues caused by high-concentration conductive particles and possesses the potential to print asymmetric electrical Janus fibers.[69,70] Furthermore, cryobioprinting synergistically utilizes phase transition mechanisms to freeze and shape ultra-soft pure conductive polymers while endowing the scaffolds with highly interconnected hierarchical porous networks.[71-73] In the dimension of enhancing resolution, EF-driven electrohydrodynamic printing has broken the

physical limits of traditional extrusion; its Taylor cone jet mechanism enables the sub-micron, ultra-high-precision deposition of highly viscous conductive bioinks.[74]

Moreover, to break through the bottlenecks of singular physical mechanisms, hybrid bioprinting—which deeply integrates printing modules with complementary advantages—has become a prominent trend. For instance, the extrusion-inkjet hybrid system effectively combines the advantages of extrusion-based technology in rapidly constructing large-volume load-bearing frameworks with the strengths of inkjet printing in localized high-resolution microdroplet patterning.[75] Meanwhile, the extrusion-photocuring hybrid strategy enables the synchronous fabrication of opaque conductive networks and high-precision insulating matrices.[76] These hybrid manufacturing paradigms achieve the synergistic fabrication of macroscopic structural support and microscopic electrical/biological interfaces on the same platform, effectively overcoming the performance limitations of traditional single processes.[77]

Simultaneously, several disruptive emerging biofabrication technologies are reshaping the boundaries of electroactive tissue engineering. For example, volumetric bioprinting, acting as a layerless lithography technique, utilizes the principle of tomographic projection to generate complex centimeter-scale 3D physical entities in a rotating vat within tens of seconds. This not only thoroughly overcomes the major challenge of cell death caused by prolonged processing times in conventional layer-by-layer printing but also effectively prevents the gravity-induced sedimentation of high-density conductive fillers in low-viscosity bioinks.[78] On the other hand, acoustic-assisted bioprinting exhibits immense potential. Not only can it achieve completely nozzle-free droplet ejection via focused acoustic fields, fundamentally eliminating the risk of clogging by conductive particles, but more crucially, by leveraging acoustic tweezers derived from standing wave fields, it can contactlessly guide the highly ordered alignment of internal conductive nanofillers or living cells prior to the crosslinking of the bioink. This provides a revolutionary physical intervention strategy for constructing skeletal muscle and central nervous tissues equipped with highly anisotropic conductive networks.[79]

In summary, the future fabrication of electroactive biomimetic scaffolds will move beyond traditional singular processes toward a next-generation intelligent manufacturing paradigm. This paradigm features multi-scale hybridization, multi-material integration, and the incorporation of novel acoustic, optical, and electrical modulations. Together, these advances will enable the reconstruction of the complex electromechanobiological microenvironments of native tissues with unprecedented fidelity.

4. Conductive and electroactive bioinks

Within this technological framework, the bioinks serve as the fundamental carrier for building tissue constructs. During the printing process or immediately following deposition, the bioink is stabilized and solidified via physical, chemical, or photocrosslinking, thereby precisely replicating the pre-designed macroscopic geometry and microscopic network architecture.[80] To ensure that the printed tissues and organs can perform normal physiological functions, an ideal bioink must exhibit excellent rheological printability, mechanical strength comparable to that of the target tissue, and high biocompatibility.[81] Bioinks are typically formulated from hydrogel systems comprising natural biomacromolecules, synthetic polymers, or their blends. However, in regenerative strategies that incorporate the synergistic intervention of electrotherapy, conventional insulating biomacromolecules often fail to meet the functional requirements for electrical signal transduction. Consequently, developing electroactive bioinks capable of simultaneously providing structural support and electrical signal transduction has emerged as a pivotal step in advancing current 3D bioprinting technologies.[82-84] Currently, electroactive ink systems are mainly classified into passively powered conductive ink systems and self-powered ink systems.

4.1. Conductive bioinks

The performance of 3D-bioprinted electroactive constructs is highly dependent on bioink composition, which governs printing fidelity, electrical signal transduction, and the long-term viability of encapsulated cells.[83] The conductive bioinks developed to date are predominantly based on poly(3,4-ethylenedioxythiophene) polystyrene sulfonate (PEDOT:PSS), PPy, PANI, and their composites with other substances. Overall, they can be classified into three major categories: pure conductive polymer bioinks, conductive particle-loaded bioinks, and bioinks incorporating non-conductive polymers, as summarized in Table 1.

4.1.1. Pure conductive polymer bioinks

Currently, pure conductive polymer bioinks are primarily based on three major types of polymers: PEDOT:PSS, PANI, and PPy. These materials possess highly π-conjugated electronic backbones, endowing them with high intrinsic electrical conductivity and electrochemical activity.[105] Owing to their intrinsic organic nature, pure conductive polymers facilitate efficient coupling between electronic charge carriers and ionic species in interstitial fluids during charge transfer, especially when compared to

Table 1. Representative examples of polymer-based conductive bioinks, printing techniques, resolutions, and conductivity

Category	Composition	Technique	Resolution (μm)	Conductivity (S/cm)	Reference
Pure conductive polymer inks	PEDOT:PSS/DMSO	DIW	30	28	[85]
	PEDOT:PSS/DBSA	DIW	20	0.1	[86]
	PANI/DBSA	DIW	250	20	[87]
	PANI/PPY/PSS	IJP	10	–	[88]
	PEDOT:PSS/Ag	APAP(DIW)	38	4.26×10^5	[89]
Composite inks with conductive fillers	PEDOT:PSS/CNTs	DIW	100	–	[90]
	PEDOT:PSS/MXene	DIW	200–500	15.258	[91]
	PEDOT:PSS/MXene	DIW	200	1,600 ± 400	[92]
	PPY/GA	DIW	210	–	[93]
	PANI/MXene	DIW	210	1,650	[94]
	PEDOT:PSS/PEO	EHD	27.25 ± 3.76	–	[74]
	PEDOT:PSS/GelMA	DIW	120	–	[95]
	PEDOT:PSS/GelMA	2PP	100	9×10^{-4}	[96]
	PEDOT:PSS/PEGDA	SLA	–	0.055	[97]
Composite inks with non-conductive fillers	PEDOT:PSS/PVA/PAA	DIW	60	0.0443	[98]
	PEDOT:PSS/PVAF	DIW	120	1.0653 ± 0.2058	[99]
	PPY/GelMA/CS	DIW	160	797	[100]
	PPY/PLLA	DIW	260	7.5×10^{-5}	[101]
	PPY/HA	DIW	–	4.3×10^{-6}	[102]
	PANI/CNC	DIW	200	0.0335	[103]
	PANI/PEGDA	SLA	–	2×10^{-6}	[104]

Abbreviations: 2PP: Two-photon polymerization; Ag: Silver; APAP: Air pressure-assisted printing; CNC: Cellulose nanocrystal; CNTs: Carbon nanotubes; CS: Chitosan; DBSA: Dodecylbenzenesulfonic acid; DIW: Direct ink writing; DMSO: Dimethyl sulfoxide; EHD: Electrohydrodynamic printing; GA: Graphene aerogel; GelMA: Gelatin methacryloyl; HA: Hyaluronic acid; IJP: Inkjet printing; MXene: Two-dimensional transition-metal carbide, nitride, or carbonitride; PAA: Poly(acrylic acid); PANI: Polyaniline; PEDOT:PSS: Poly(3,4-ethylenedioxythiophene):poly(styrene sulfonate); PEGDA: Poly(ethylene glycol) diacrylate; PEO: Poly(ethylene oxide); PLLA: Poly(L-lactic acid); PPY: Polypyrrole; PSS: Poly(styrene sulfonate); PVA: Poly(vinyl alcohol); PVAF: Poly(vinyl alcohol) fiber; SLA: Stereolithography.

conventional inorganic metals.

Poly(3,4-ethylenedioxythiophene) polystyrene sulfonate is highly favored in 3D bioprinting due to its excellent aqueous dispersibility and biocompatibility.[106] Yuk *et al.*[85] developed a high-performance PEDOT:PSS ink capable of being printed into microstructures with high resolution and high aspect ratios. By employing a technique of lyophilization (freeze-drying) followed by solvent (water/dimethyl sulfoxide [DMSO]) redispersion, the printed polymer networks could be converted into ultrasoft and highly conductive hydrogels. These were successfully applied in the fabrication of soft neural probes, enabling precise *in vivo* electrophysiological recording of single neurons. However, to induce phase separation, conventional PEDOT:PSS printing often requires harsh post-processing steps, such as lyophilization, the use of strong solvents (e.g., DMSO), or dry annealing. This restricts its potential for in situ biological applications. To overcome this barrier, Zhang *et al.*[86] utilized dodecylbenzenesulfonic acid (DBSA) to screen the electrostatic interactions between PEDOT and PSS, successfully inducing the physical crosslinking of exposed poly(3,4-ethylenedioxythiophene) (PEDOT) chains via π – π stacking at room temperature. They developed a fully injectable, self-healing soft PEDOT:PSS hydrogel,

significantly broadening the application prospects of pure conductive hydrogels in minimally invasive biotherapies and *in situ* electrotherapeutic repair.

Polyaniline is inherently difficult to process using additive manufacturing owing to its poor solubility and lack of thermoplasticity. To overcome these limitations, Menzel *et al.*[87] proposed a novel extrusion-based printing method leveraging a thermal doping process. They combined low-conductivity emeraldine base (termed PANI-EB) with DBSA; subsequent heating induced its transformation into highly conductive emeraldine salt (termed PANI-ES), simultaneously improving the rheological properties of the ink to suit extrusion processing, achieving a high conductivity of up to 20 S/cm.

Pure PPy frequently induces severe nozzle clogging due to its poor aqueous dispersibility and strong propensity for agglomeration. To achieve high-precision micro-patterning, Zea *et al.*[88] specifically engineered a composite conductive ink that integrates PANI and PPy with the polyelectrolyte sodium polystyrene sulfonate (PSS). The incorporation of PSS precisely tuned the surface tension and rheological properties of the PANI/PPy blend, thereby eliminating the nozzle clogging issue. Furthermore, it substantially enhanced the electrochemical stability of the resulting material.

4.1.2. Conductive bioinks incorporating conductive particles

Integrating conductive polymers with additional conductive fillers (e.g., Ag, CNTs, two-dimensional transition-metal carbide [MXene], and graphene aerogel) can substantially enhance the overall electrical conductivity. These fillers typically possess abundant functional groups or surface charges, enabling self-assembly with intrinsically conductive polymers via hydrogen bonding, $\pi - \pi$ stacking, and electrostatic interactions of the bioink.

To enhance the electrical conductivity of PEDOT:PSS, Yang *et al.*[90] introduced CNTs into the bioink. Electrodes printed using this CNT-blended ink not only exhibited improved mechanical strength but also featured a dense CNT network that provided high-speed pathways for electron transport. Consequently, the areal capacitance of the electrodes reached 990 mF/cm^2, which is 2.33 times that of pure PEDOT:PSS. Liu *et al.*[91] incorporated hydrophilic two-dimensional (2D) Ti_3C_2 MXene nanosheets into PEDOT:PSS. The functional groups on the MXene surface established strong electrostatic and hydrogen-bonding interactions with PEDOT:PSS, yielding a printable bioink with an electrical conductivity as high as 1,525.8 S/m.

Two-dimensional carbon-based materials, such as graphene oxide (GO), are frequently utilized to improve the printability and porosity of conductive polymers, owing to their ultra-high specific surface area and mechanical strength. He *et al.*[93] designed a GO/PPy composite ink specifically tailored for direct ink writing 3D printing. The incorporation of GO nanosheets not only endowed the PPy ink with excellent shear-thinning behavior and self-supporting extrusion capabilities but also, following printing, lyophilization, and chemical reduction, facilitated the successful construction of a graphene aerogel/PPy scaffold with a hierarchical porous structure.

Conventionally, 3D-printed PANI electrodes typically suffer from low active material loading and poor charge transport. To address this challenge, Meng *et al.*[94] developed a highly concentrated MXene/PANI gel ink via a solvent-assisted self-assembly strategy. This molecular-level synergy between 2D and 0D materials effectively overcame the physical drawback of PANI's propensity for agglomeration. Furthermore, without the requirement of any insulating additives, it endowed the ink with superior shear-thinning and self-supporting properties, ultimately yielding a 3D-printed hierarchical porous gel network with an outstanding electrical conductivity of up to 1,650 S/cm.

4.1.3. Composite conductive bioinks incorporating non-conductive polymers

Although pure conductive inks and bioinks loaded with conductive particles possess excellent electrical conductivity, their inherent rigidity and brittleness restrict their biomedical applications. To overcome these limitations, conductive materials are often incorporated into non-conductive polymers, including gelatin methacryloyl (GelMA), poly(ethylene glycol) diacrylate (PEGDA), and poly(vinyl alcohol) (PVA), to form composite bioinks. Such formulations enhance printability, rheological behavior, and biocompatibility while maintaining adequate electrical conductivity.

For instance, to overcome the inherent instability of processing conductive polymers via electrohydrodynamic printing, Chang and co-workers[74] introduced high-molecular-weight poly(ethylene oxide) into PEDOT:PSS as a rheological modifier, which substantially elevated the viscosity and surface tension of the ink, thereby improving the printability of the PEDOT:PSS formulation. Zhang *et al.*[98] incorporated PVA and poly(acrylic acid) (PAA) into PEDOT:PSS. Leveraging the strong electrostatic interactions between PEDOT:PSS and the abundant free hydroxyl and carboxyl groups of PVA/PAA, they substantially increased the viscosity of the blended ink. Experimental testing demonstrated a shear adhesive strength exceeding 28.5 kPa on porcine skin surfaces.

In electroactive tissue engineering, biocompatibility is

as important as electrical conductivity in bioink design. The incorporation of natural non-conductive polymers can provide a biomimetic ECM-like microenvironment that supports the survival, proliferation, and function of encapsulated cells. For example, Serafin *et al.*[102] found that uniformly dispersing PPy nanoparticles within gelatin and high-molecular-weight hyaluronic acid formed a biomimetic macromolecular network, effectively mitigating the inherent drawback of poor cell adhesion typically associated with pure PPy. While the introduction of insulating macromolecules inevitably leads to a decline in ink conductivity, Wan *et al.*[99] discovered a unique phenomenon when incorporating poly(vinyl alcohol-co-ethylene) (PVAF) into PEDOT:PSS. Beyond merely increasing the ink's viscosity and optimizing its shear properties, the abundant polar hydroxyl groups in PVAF acted as secondary dopants for PEDOT:PSS. This promoted the phase separation of PEDOT and PSS via the charge screening effect, thereby densifying the conductive network. Consequently, the composite ink achieved a high electrical conductivity exceeding 100 S/m, despite the presence of a substantial insulating matrix.

Furthermore, to meet the requirements of photocuring-based bioprinting, photo-crosslinkable non-conductive polymers are frequently integrated into pure conductive inks. For example, incorporating GelMA into PEDOT:PSS endows the ink with excellent visible-light crosslinking capability (450–550 nm). Similarly, adding PEGDA to PEDOT:PSS or PANI enables photocurable 3D bioprinting, with subsequent UV post-curing increasing the conversion rate of PEGDA to over 80%.[97,104]

In summary, within the realm of electroactive tissue engineering, there is no single material or process that is universally suitable for all clinical scenarios. Future applications should be guided by the physiological characteristics of the targeted tissues and rationally select the most compatible 3D printing modalities and conductive ink formulations tailored to specific clinical demands. Only through the integration of materials, architectures, and biological functions can optimal conductive scaffolds be successfully printed, thereby fully unleashing the potential of electrophysiological interventions in tissue therapy.

4.2. Electroactive bioinks

Electroactive bioinks represent a shift from passive charge conduction to active in situ power generation by incorporating energy-harvesting and conversion components into polymer or hydrogel matrices with suitable printing properties. Based on their underlying energy conversion mechanisms, this section highlights several representative electroactive bioink systems, including self-powered piezoelectric/triboelectric, magnetoelectric bioinks that harvest mechanical energy, as well as metabolically driven living bio-batteries and optoelectronic hybrid systems (Table 2).

4.2.1. Self-powered piezoelectric bioink systems

Piezoelectric materials contain spontaneously polarized electric dipoles that can intrinsically generate electrical signals upon experiencing mechanical deformation. Common piezoelectric materials include polyvinylidene fluoride (PVDF), barium titanate ($BaTiO_3$), and zinc oxide (ZnO). However, pure single-component materials are often difficult to utilize directly as bioinks for printing electroactive scaffolds; they typically require further optimization through modification or composite strategies.

Polyvinylidene fluoride is highly favored in flexible 3D printing due to its exceptionally high piezoelectric coefficient and outstanding flexibility. Liang *et al.*[107] developed a high-performance 3D-printable PVDF composite hydrogel ink capable of fabricating orthogonal grid dressings with vertically interconnected microporous structures. By employing sodium alginate (SA) for hydrophilic modification, the printed polymer network can be transformed into a highly absorbent and flexible piezoelectric scaffold, which was successfully applied to promote scarless wound healing. To address the lack of continuous mechanical stimulation for piezoelectric scaffolds *in vivo*, Li *et al.*[108] proposed an innovative strategy that ingeniously couples the piezoelectric effect with the shape-memory effect. They integrated annealing-induced, high β-phase PVDF nanofibers with a 3D-printed shape-memory polyurethane framework to construct a smart bone repair scaffold with "two-stage *in situ* self-powering" capabilities. Triggered by body temperature, this scaffold undergoes shape deformation, thereby generating a micro-high-voltage electrostatic field.

$BaTiO_3$ is a classical ceramic piezoelectric material, often utilized in piezoelectric scaffolds due to its excellent piezoelectric properties and low toxicity. However, owing to its lack of thermoplasticity and high susceptibility to particle agglomeration, achieving high-precision cell-laden bio-additive manufacturing using traditional methods is extremely challenging. To overcome this limitation, Li *et al.*[109] proposed a novel photo-crosslinkable bioprinting method based on DLP. They combined polyethylene glycol (PEG)-surface-modified $BaTiO_3$ nanoparticles (PEG@BT) with GelMA. This surface coating effectively prevented the agglomeration of inorganic particles while concurrently improving the light transmittance and dispersibility of the ink, making it highly suitable for DLP processing. Meanwhile, Polley *et al.*[111] mixed $BaTiO_3$ with

Table 2. Representative examples of electroactive systems based on bioinks, printing techniques, output voltage, and power

Category	Composition	Technique	Output voltage (V)	Output power (W/m²)	Reference
Piezoelectric systems	PVDF/SA/ZnO	DIW	–	–	[107]
	SMPU	DIW	340	–	[108]
	GelMA/$BaTiO_3$	DLP	0.02	–	[109]
	PCL/$BaTiO_3$	FFF	–	–	[110]
	PEMA/HA/$BaTiO_3$	DIW	–	–	[111]
	PLA/KNN	DIW	17.9	–	[112]
	SA/PAM/PHBV	SLA	0.4	–	[113]
Triboelectric systems	PVDF	FFF	260	690	[114]
	PDMS/PVDF/$FAPbI_3$	DIW	392	25,870	[115]
	HEAA/PEGDA/SBMA	LCD	802	48.4	[116]
	ARO/AESO	DIW	22	0.34	[117]
	MXene	DIW	–	0.8166	[118]
	PGS/PEDOT:PSS/NaCl	DIW	5	–	[119]
Magnetoelectric systems	PCL/$CoFe_2O_4$	DIW	–	–	[120]
	4-HBA/NCs	DLP	–	–	[121]
	GelMA/MENPs	2PP	–	–	[122]
Bio-battery systems	Alginate	DIW	–	13	[123]
	Alginate/GO/Bacterium	DIW	–	8.13	[124]
	CNC/*Saccharomyces cerevisiae*	DIW	0.6	12.54	[125]
Optoelectronic systems	PPY/GelMA/CS	DIW	160	797	[126]

Abbreviations: 2PP: Two-photon polymerization; 4-HBA: 4-Hydroxybutyl acrylate; AESO: Acrylated epoxidized soybean oil; ARO: Acrylated rapeseed oil; $BaTiO_3$: Barium titanate; CNC: Cellulose nanocrystal; $CoFe_2O_4$: Cobalt ferrite; CS: Chitosan; DIW: Direct ink writing; DLP: Digital light processing; $FAPbI_3$: Formamidinium lead iodide; FFF: Fused filament fabrication; GelMA: Gelatin methacryloyl; GO: Graphene oxide; HA: Hydroxyapatite; HEAA: N-hydroxyethyl acrylamide; KNN: Potassium sodium niobate; LCD: Liquid-crystal display; MENPs: Magnetoelectric nanoparticles; MXene: Two-dimensional transition-metal carbide, nitride, or carbonitride; NaCl: Sodium chloride; NCs: Nanocookies; PAM: Polyacrylamide; PCL: Polycaprolactone; PDMS: Polydimethylsiloxane; PEDOT:PSS: Poly(3,4-ethylenedioxythiophene):poly(styrene sulfonate); PEGDA: Poly(ethylene glycol) diacrylate; PEMA: Poly(ethyl methacrylate); PGS: Poly(glycerol sebacate); PHBV: Poly(3-hydroxybutyrate-co-3-hydroxyvalerate); PLA: Poly(lactic acid); PPY: Polypyrrole; PVDF: Poly(vinylidene fluoride); SA: Sodium alginate; SBMA: Sulfobetaine methacrylate; SLA: Stereolithography; SMPU: Shape-memory polyurethane; ZnO: Zinc oxide.

large-particle-size hydroxyapatite powder, ingeniously utilizing hydroxyapatite to improve the flowability of the ceramic powder on the print bed. Following high-temperature sintering and polarization, they obtained a biomimetic porous scaffold with a piezoelectric coefficient (approximately 3.08 pC/N) that perfectly matches the physiological properties of natural dry bone.

Driven by the requirements of *in vivo* applications, the development of biodegradable electroactive inks has emerged as a significant trend. Because of their strong hydrophobicity, pure biodegradable piezoelectric polyesters such as poly(3-hydroxybutyrate-co-3-hydroxyvalerate) (PHBV) are highly incompatible with hydrogel matrices, which can easily lead to phase separation and nozzle clogging. To achieve high-precision multi-layer printing, Huang *et al.*[113] specifically designed a unique ternary mixed solvent system integrating water, N,N-dimethylformamide, and dichloromethane. By optimizing the miscibility and rheology of hydrophobic PHBV and hydrophilic SA/polyacrylamide ( ) networks,

this solvent system eliminated printing phase separation and enabled the fabrication of a piezoelectric gradient for dynamically adaptive tissue remodeling.

4.2.2. Self-powered triboelectric bioink systems

Unlike the piezoelectric effect, which depends on the crystal structure of materials, the triboelectric nanogenerator (TENG) utilizes the coupling effect of contact electrification and electrostatic induction, enabling the efficient harvesting of energy from ultra-low-frequency biomechanical movements. Because their fundamental mechanism relies on differences in electron affinity, self-powered inks require the precise pairing of polar materials strictly according to the triboelectric series to facilitate effective charge transfer.

Poly(vinylidene fluoride) is frequently utilized as a classical tribo-negative matrix in 3D printing owing to its extraordinarily strong electron-withdrawing capability. However, pure PVDF often struggles to achieve a high content of electroactive phases during conventional printing and processing. Zain Karimy *et al.*[115] developed a high-performance PVDF composite ink capable of fabricating porous dielectric films. By employing direct ink writing and introducing polymorphous perovskite nanofillers, they robustly induced the phase transition of PVDF from the non-polar α phase to the highly electroactive β phase, thereby significantly enhancing the material's triboelectric positivity and dielectric constant. Furthermore, Meena *et al.*[114] utilized the fused filament fabrication process to naturally induce the polar crystalline phase of PVDF under elevated temperatures and shear forces. Simultaneously, by leveraging the microscopic surface roughness generated by the nozzle movement, they substantially increased the triboelectric contact area, achieving a hybrid enhancement of both piezoelectric and triboelectric effects.

Traditional TENG materials are highly susceptible to charge leakage and subsequent failure in high-humidity environments, such as body fluids. To overcome this environmental limitation, Zhuo *et al.*[116] presented a printable strategy that leverages ambient moisture to enhance output by integrating polar hydrophilic networks via liquid crystal display 3D printing. They designed a superhydrophilic photo-curable resin ink by introducing zwitterionic species (sulfobetaine methacrylate) into a poly(N-hydroxyethyl acrylamide) polymer network. The polar functional groups of this ink can firmly trap free water molecules from the air and convert them into bound water, completely resolving the issue of charge leakage under high humidity and achieving a multifold leap in electrical output even at an extreme relative humidity of 90%.

For *in vivo* tissue engineering, traditional rigid triboelectric materials are highly prone to triggering inflammation, which restricts their application in *in vivo* repair. To overcome this obstacle, Ma *et al.*[119] and Luo *et al.*[127] employed biodegradable poly(glycerol sebacate) with a biomimetic modulus as a tribo-negative matrix and homogeneously incorporated highly conductive, tribo-positive PEDOT:PSS to develop a composite ink exhibiting shear-thinning characteristics. Combining 3D printing with particulate leaching techniques, they constructed a 3D framework rich in hydrophobic micropores. When subjected to compression *in vivo*, the inner walls of these pores can undergo highly efficient contact-separation electrification. This architecture was successfully applied to accelerate endochondral ossification repair and enable non-contact wireless ES therapy.

4.2.3. Other emerging electroactive bioink systems

Beyond piezoelectric and triboelectric systems that rely on mechanical deformation, 3D-printed electroactive bioinks are expanding toward multi-physics field responsiveness and purely endogenous metabolism. In recent years, through meticulous material formulation and rheological design, researchers have ingeniously integrated magnetic nanoparticles, living microbial systems, and micro/nano solid-state devices into printable polymer matrices. This has led to the development of novel composite inks, including magnetoelectric, biological fuel cell, and optoelectronic heterogeneously integrated systems.

Incorporating inorganic magnetoelectric nanomaterials into polymer matrices is a crucial approach to achieving magnetically driven wireless power generation. Cobalt ferrite ($CoFe_2O_4$) is one of the most classical magnetoelectric materials; however, cobalt ions exhibit inherent heavy metal toxicity. To overcome this materials science obstacle, Kaviani *et al.*[120] specifically designed a magnetic nanocomposite ink with a core-shell architecture. Utilizing a sol-gel method, they coated a highly magnetically responsive $CoFe_2O_4$ core with a Mg_2SiO_4 silicate shell, subsequently melt-blending it with polycaprolactone (PCL). This endowed the printed composite network with excellent hydrophilicity and auto-buffered degradation capabilities, leading to its successful application in bone tissue regeneration strategies. Conversely, Fang *et al.*[121] selected carbon-based magnetized nanocookies (NCs) with a porous structure as the magnetoelectric material. They dispersed the magnetoelectric particles in 4-hydroxybutyl acrylate and leveraged the rapid localized crosslinking characteristics of DLP 3D printing to precisely expose the NCs at the photopolymerized edges on the gel surface. This "surface exposure" strategy completely eliminated the charge-shielding effect of the polymer network, enabling

wireless magnetically induced microcurrents to stimulate cells at the material–cell interface.

To achieve entirely endogenous, passive self-powering, living bio-battery inks that utilize microbial chemical metabolic energy for continuous power generation have emerged as a novel trend. The core design of such composite inks lies not only in maintaining cell viability but also in constructing an efficient metabolic symbiotic network and a cell-electrode electron transfer pathway. Regarding symbiotic metabolic power generation, Wang *et al.*[124] incorporated insulating GO into an alginate composite matrix and embedded bacteria. After printing and molding, these exoelectrogenic bacteria could not only continuously metabolize to generate electrons but also act as reducing agents to biologically reduce the GO *in situ* into highly conductive reduced GO. This living battery exhibited exceptional self-charging capabilities and a Coulombic efficiency of up to 99.5%, with its continuously generated metabolic microcurrents being successfully applied to drive *in vivo* neural ES. For those seeking completely metal-free and environmentally biodegradable energy storage systems, Reyes *et al.*[125] formulated fungal battery inks for anodes and cathodes based on purely plant-derived cellulose. Driven solely by biochemical reactions, this 3D-printed fungal battery could generate a maximum power density of 12.54 μW/cm^2 per single cell and is fully biodegradable in the natural environment after disposal.

Traditional optoelectronic polymer inks typically rely on the chemical synthesis of complex organic conjugated molecules or inorganic semiconductors, which inevitably introduces issues like cytotoxicity and stringent processing conditions. Ershad *et al.*[126] abandoned the molecular-level optoelectronic modification of inks, proposing an optoelectronic heterogeneous integration bioink formulation strategy. By uniformly suspending micro-solar cells, fabricated via micro/nano processing, as micro-fillers directly into a GelMA matrix, they constructed a novel photoelectrically active bioink. The printed scaffolds' ability to instantaneously generate weak photocurrents under illumination provides a completely new paradigm for achieving non-invasive optically controlled ES, shifting the focus from chemical synthesis to the physical integration of microelectronic devices.

Three-dimensionally printed bioinks are undergoing a profound evolution from single materials to multi-dimensional composites and cross-scale integration. Current research has successfully overcome traditional limitations in processing precision, polarization conditions, and biocompatibility through rheological tuning, phase-interface engineering, and process adaptation. This progress spans diverse energy systems, from piezoelectric and triboelectric platforms to magnetoelectric, bio-metabolic, and optoelectronic networks. Looking ahead, the development of smart bioinks that combine high energy efficiency, long-term stability *in vivo*, and complete biodegradability will remain a central focus.

5. Applications of 3D-printed conductive scaffolds in tissue engineering

Three-dimensionally printed conductive scaffolds establish a unique physical interface for the profound integration of exogenous ES with the impaired tissue microenvironment. By leveraging their high-resolution customizability in spatial topology alongside superior electrochemical activity, these scaffolds precisely recapitulate the natural ECM. Consequently, they provide both a structural framework and an electrical signal transduction network to support ideal cell-matrix interactions. Facilitated by these bridging conductive networks, ES can modulate critical cellular behaviors, such as galvanotaxis, proliferation, and directed differentiation, which are central to accelerating tissue remodeling and regeneration. The integration of conductive or electroactive scaffolds with ES represents a powerful strategy for overcoming the limitations of conventional passive scaffolds and enhancing tissue regeneration. This chapter reviews recent advances in the application of this synergistic approach to wound healing, neural regeneration, bone repair, muscle and cardiac tissue reconstruction, emphasizing the underlying mechanisms and its potential to accelerate functional tissue restoration.

5.1. Wound repair

The mechanism of wound healing is a highly orchestrated cascade comprising hemostasis, inflammation, proliferation, and remodeling. During natural healing, an endogenous bioelectric field (approximately 10–60 mV) is generated at the wound margins to drive cellular migration toward the wound bed.[128] However, in instances of extensive trauma, severe burns, or chronic diabetic ulcers, this endogenous EF progressively attenuates or completely dissipates. This disruption results in delayed cell migration, disordered collagen deposition, and the formation of severe pathological scars.[129,130] Integrating 3D bioprinting technology with ES not only facilitates the precise reconstruction of the impaired electrophysiological microenvironment using conductive scaffolds but also guides tissue regeneration through customized macro- and micro-spatial architectures. Consequently, recent cutting-edge research has yielded breakthrough advancements in the realm of wound repair.[131,132]

5.1.1. Skin wounds

Skin wounds are one of the most common bodily injuries.

While healthy individuals typically achieve spontaneous healing within a week, diabetic wounds are notoriously recalcitrant to self-healing. In these hard-to-heal diabetic wounds, bacterial eradication serves as a crucial prerequisite for successful wound closure. To achieve optimal bactericidal effects, Kumi *et al.*[133] integrated 3D bioprinting technology with intrinsically antimicrobial materials. As illustrated in Figure 4a, following 3D printing, the scaffold underwent *in situ* quaternization using glycidyltrimethylammonium chloride to convert dibutyrylchitin into quaternized chitosan (CS), which was subsequently blended with PEDOT:PSS to fabricate a flexible 3D-printed electrode. Leveraging the abundant cationic groups on its polymer chains, this electrode directly adsorbed and ruptured negatively charged bacterial membranes via robust electrostatic interactions. Upon the superimposition of an external micro-pulsed EF, the synergistic effect between this intrinsic electrostatic field and the applied EF boosted the eradication rate of methicillin-resistant *Staphylococcus aureus* to over 98% in an *in vivo* diabetic infection model. This synergistic intervention attenuated the localized inflammatory response and propelled the wound toward epithelialized closure within 14 days.

Conventional exogenous electrotherapy relies heavily on external power sources, which severely restrict patient mobility. To address this, Liang *et al.*[107] fabricated a ZnO-modified PVDF/SA composite hydrogel using 3D bioprinting, harnessing the piezoelectric effects of ZnO and PVDF to deliver wireless ES. During the hemostasis and inflammation phases, the 3D-printed porous network rapidly absorbed large volumes of wound exudate, undergoing significant vertical swelling; the resulting volumetric deformation stress stimulated the PVDF to generate piezoelectric microcurrents. Subsequently, in the proliferation and remodeling phases, as the wound formed an eschar and exudation diminished, the horizontal friction generated between the dressing and the skin due to daily human activities served equally well as a source of ES. By orchestrating a cascade of cellular migration, vascularization, collagen remodeling, and related growth factor expression throughout the healing process, this dynamic system substantially accelerated wound healing and prevented the formation of scar tissue within two weeks (Figure 4b).

High-quality wound regeneration relies not only on cellular proliferation but also on the highly ordered arrangement of the ECM. Lee *et al.*[134] utilized DLP technology to precisely engineer micro-topographies on the surface of conductive dressings to direct cellular behaviors. As depicted in Figure 4c, they employed a photosensitive, non-conductive polymer, GelMA, as the matrix, doped with the conductive polymer PEDOT:PSS. The incorporation of PEDOT:PSS not only endowed the hydrogel with excellent electrical conductivity but also substantially enhanced its mechanical tensile strength through electrostatic interactions between the PSS chains and the gelatin backbone. The conductive microgrooved scaffolds, coupled with ES, markedly activated the PI3K/AKT and MAPK/ERK signaling pathways in fibroblasts. This process significantly upregulated the secretion of fibroblast growth factors and collagen, thereby expediting wound repair.

Electrical stimulation devices and electrodes that directly contact the wound bed may increase the risk of infection and cause secondary tissue damage during removal. To circumvent this, Luo *et al.*[127] developed a completely soft, biodegradable TENG based on PEDOT:PSS using 3D printing technology (Figure 4d). This device overcame conventional spatial contact limitations by utilizing limb movement to trigger the contact and separation of internal micropores. The resulting alternating spatial EF could induce the formation of an electric double layer in the interstitial fluid at a distal distance of up to 44 mm from the wound. Remarkably, these nonadjacent wireless-induced microcurrents still managed to boost early-stage wound repair efficiency by over 336% and substantially promoted collagen deposition and angiogenesis.

5.1.2. Mucosal wound

Wound repair of luminal mucosa confronts extreme microenvironmental challenges completely distinct from those of the epidermal surface, including continuous fluid flushing and high-frequency dynamic mechanical stretching. Conventional static, insulating dressings frequently encounter adhesion failure or suboptimal histological remodeling in these regions, making the repair of internal mucosal wounds particularly challenging.

Nie *et al.*[135] developed a natural macromolecular composite formulation based on SA and hyaluronic acid, utilizing 3D bioprinting technology to construct a bilayered endometrial construct for treating endometrial injury. By depositing endometrial epithelial cells with high structural fidelity on the upper layer to reconstruct a dense mucosal barrier and printing endometrial stromal cells within the underlying grid to induce vascularization, this strategy faithfully recapitulated the delicate hierarchical microenvironment of the endometrium. In a rat model of partial full-thickness uterine excision, the implantation of this 3D-printed bilayered endometrial construct demonstrated substantial regenerative advantages 90 days post-surgery. Figure 5a illustrates the conceptual model

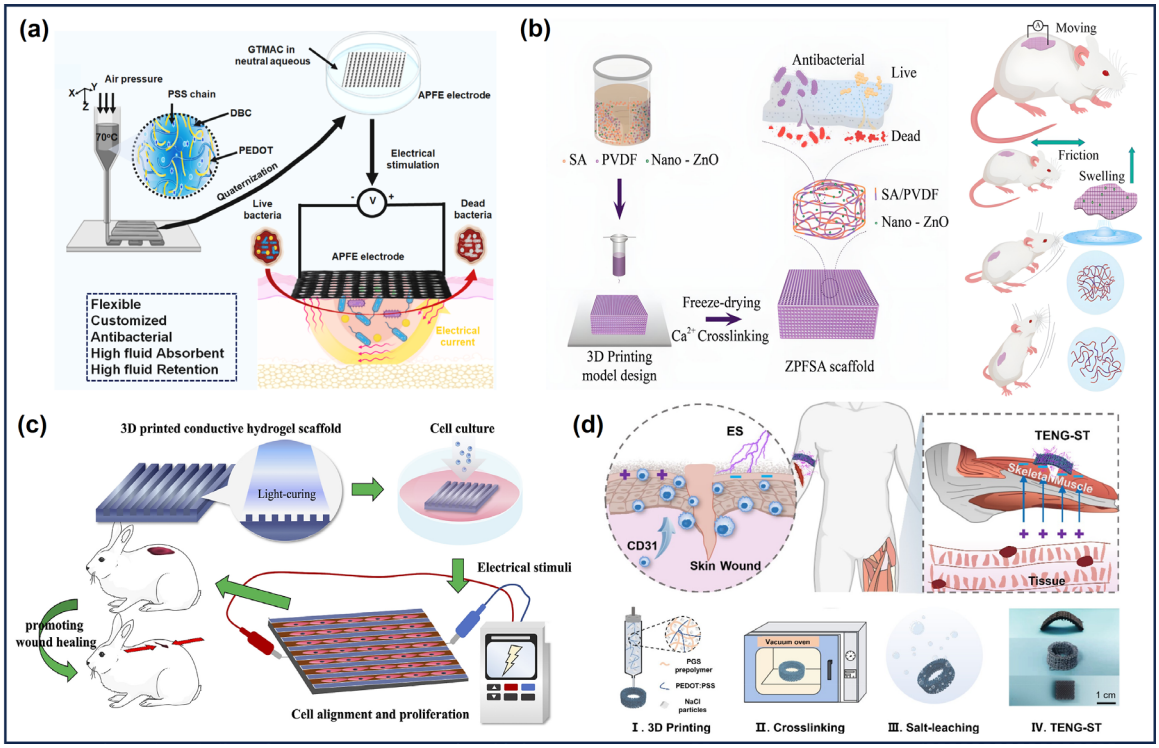

Figure 4. Applications of 3D-printed electroactive scaffolds synergized with electrical stimulation for skin wound healing. (a) Design and fabrication principles of the antimicrobial flexible electrode. The scaffold is extruded using a bioink composed of PEDOT:PSS and dibutyrylchitin. Adapted with permission from Kumi *et al.*[133] Copyright © 2025, Elsevier B.V. (b) The fabrication process and pro-healing mechanism of the 3D-printed piezoelectric hydrogel scaffold. Reprinted with permission from Liang *et al.*[107] Copyright © 2022, American Chemical Society. (c) A conductive hydrogel scaffold with microgrooved topography precisely engineered via digital light processing printing. Reprinted with permission from Lee *et al.*[134] Copyright © 2022, Elsevier B.V. (d) Schematic illustration of PEDOT:PSS-based 3D printing for tissue repair. Reprinted with permission from Luo *et al.*[127] Copyright © 2023, American Chemical Society.

Abbreviations: APFE: Antimicrobial porous flexible hydrogel electrode; DBC: Dibutyrylchitin; ES: Electrical stimulation; GTMAC: Glycidyltrimethylammonium chloride; PEDOT: Poly(3,4-ethylenedioxythiophene); PEDOT:PSS: Poly(3,4-ethylenedioxythiophene):poly(styrene sulfonate); PSS: Poly(styrene sulfonate); PVDF: Poly(vinylidene fluoride); PVP: Polyvinylpyrrolidone; SA: Sodium alginate; TENG-ST: Triboelectric nanogenerator-based stimulator; ZPFS: ZnO/PVDF/SA scaffold.

of this endometrial construct alongside a comparison of post-operative wound healing.

Oral ulcers represent a prevalent type of oral mucosal trauma. Targeting oral mucosal repair, Zhou *et al.*[136] developed a conductive PAM/SA crosslinked hydrogel composite containing reduced GO, as depicted in Figure 5b. Exhibiting inherent antibacterial, anti-inflammatory, and antioxidant properties, this composite acts as an electrical bridge that transforms the short circuit at the injury site into an intact circuit. This transformation effectively stimulates adjacent fibroblasts to secrete growth factors, thereby accelerating tissue regeneration. Evaluated in a rat model of full-thickness infected buccal mucosa defects, this hydrogel demonstrated exceptional anti-inflammatory and pro-healing efficacy, achieving rapid, scarless, and complete wound closure within seven days. This substantially enhances patient treatment comfort and compliance, providing a highly promising research avenue for oral mucosal repair.

For the mucosa of hollow organs with stringent fluid storage and anti-leakage requirements, simple hydrogels struggle to withstand tremendous dynamic tension. A recent strategy utilized a natural bladder acellular matrix featuring a waterproof barrier and tensile properties as the substrate. A conductive micro-network of GelMA-chitin nanocrystals doped with 2D MXene nanosheets was subsequently 3D-bioprinted onto its surface. Figure 5c$_{I}$ shows the morphologies of the printed scaffolds at different doping ratios. Under the stimulation of an optimized 400 mV alternating micro-EF, the conductive network substantially enhanced the paracrine activity (e.g., VEGF and nerve growth factor [NGF] secretion) of the loaded adipose-derived stem cells. This electromechanical synergistic intervention guided the dense regeneration of the detrusor muscle and the continuous reconstruction of the AE1/AE3-positive urothelial barrier. Concurrently, it

induced the ingrowth of microvessels and nerve endings, achieving a bidirectional restoration of both the anti-leakage and autonomic contraction functions of the luminal mucosa, thus pioneering a novel pathway for bladder defect repair (Figure 5c$_{II}$ and 5c$_{III}$).[137]

Current research on 3D-printed electroactive scaffolds for wound repair mainly focuses on basic observations. Poor understanding of how electrical signals regulate cellular responses, coupled with the absence of standardized stimulation protocols for field strength, frequency, and timing, makes cross-study comparison difficult. Most designs target skin wounds and have not adequately addressed mucosal challenges such as fluid flushing, enzymatic degradation, and mechanical strain. Future priorities include elucidating molecular pathways, developing closed-loop adaptive systems, and rationally integrating antibacterial, conductive, topographical, and biodegradable functions.

5.2. Neural repair

The nervous system serves as the core information network responsible for maintaining somatic perception, motor functions, and homeostatic control. However, neural tissue is highly vulnerable to irreversible damage caused by mechanical trauma, iatrogenic surgical injuries, and metabolic diseases. Central nervous system (CNS) injuries often result in the permanent loss of motor and sensory functions below the level of the lesion, accompanied by severe autonomic dysfunction.[138] Conversely, peripheral nervous system (PNS) injuries lead to sensory deficits

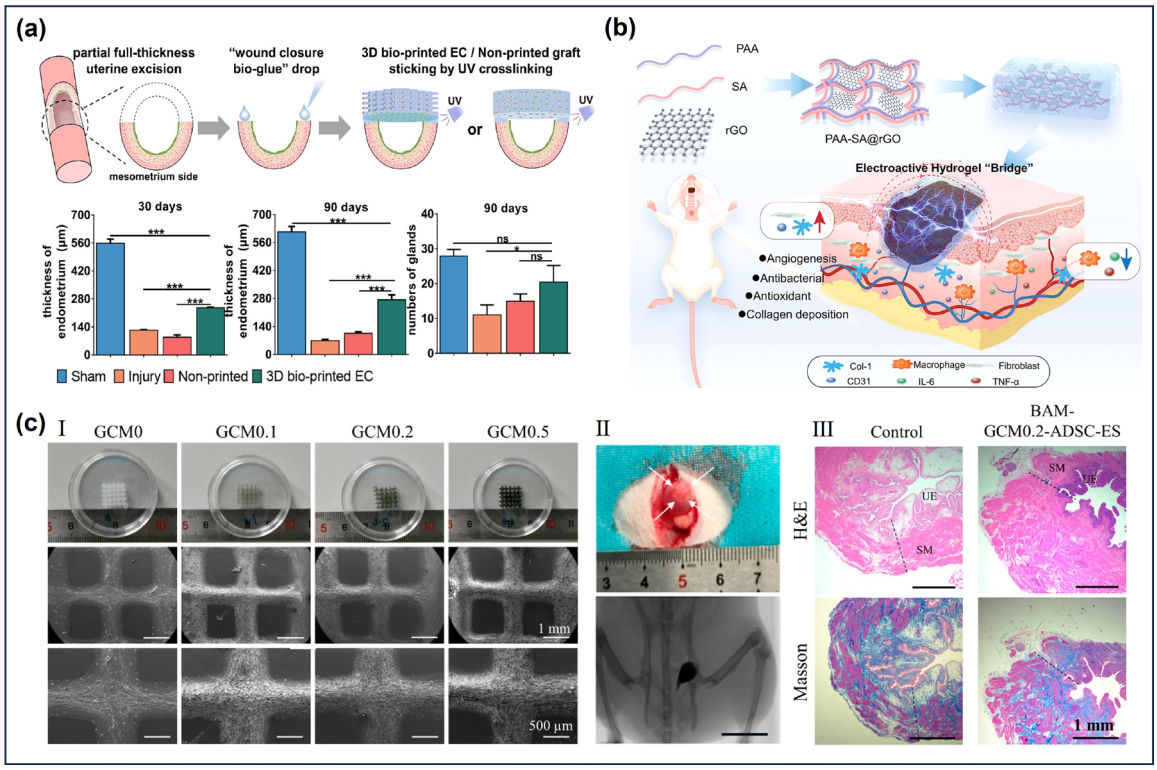

Figure 5. Applications of 3D-printed electroactive scaffolds synergized with electrical stimulation for mucosal tissue regeneration. (a) Schematic illustration of a 3D bio-printed bilayered endometrial construct for restoring the injured endometrium and the comparison at 30 and 90 days post-operation. Reprinted with permission from Nie *et al.*[135] Copyright © 2023, Elsevier Ltd. (b) Schematic illustration of the synthesis of the PAA/SA/rGO-based conductive composite hydrogel and its mechanism for accelerating oral mucosal ulcer healing. Reprinted with permission from Zhou *et al.*[136] Copyright © 2024, Wiley-VCH GmbH. (c) Systematic study of 3D-bioprinted decellularized matrix-based conductive patches for bladder repair in rats. (I) Morphologies of the 3D-bioprinted conductive networks with varying MXene doping ratios. (II) Schematic of the bladder patch for morphological bladder repair. (III) Schematic diagram comparing the therapeutic outcomes of bladder tissue regeneration. Reprinted with permission from Ling *et al.*[137] Copyright © 2024, American Chemical Society.

Abbreviations: ADSC: Adipose-derived stem cell; BAM: Bladder acellular matrix; ChiNC: Chitin nanocrystal; Col-1: Collagen type I; EC: Endometrial construct; ES: Electrical stimulation; GCM: GelMA/ChiNC/MXene bioink; GelMA: Gelatin methacryloyl; H&E: Hematoxylin and eosin; IL-6: Interleukin-6; Masson: Masson's trichrome staining; MXene: Titanium carbide MXene; ns: Not significant; PAA: Poly(acrylic acid); PAA-SA@rGO: Poly(acrylic acid)/sodium alginate hydrogel containing reduced graphene oxide; rGO: Reduced graphene oxide; SA: Sodium alginate; SM: Smooth muscle; TNF-α: Tumor necrosis factor-alpha; UE: Uroepithelium.

or neuropathic pain.[139] Consequently, the high-quality reconstruction of neural pathways holds immense medical significance. In recent years, the therapeutic paradigm for nerve defects has gradually shifted from passive structural bridging methods, such as conventional direct suturing and autografting, toward cutting-edge strategies that integrate smart scaffolds with active physical interventions based on photoelectric, magnetoelectric, and piezoelectric effects.[140-143] Against this backdrop, the convergence of 3D bioprinting technology and ES paves a highly promising new avenue for the regenerative repair of complex nerve injuries.

5.2.1. Central nervous system repair

In early explorations of remodeling the CNS microenvironment using conductive scaffolds, carbon-based nanomaterials demonstrated exceptional potential. Lee *et al.*[144] utilized SLA 3D printing technology to uniformly dope aminated multi-walled carbon nanotubes (MWCNTs) into a PEGDA hydrogel, thereby constructing a conductive neural scaffold with high-fidelity porous architectures. The Young's modulus of this composite scaffold reached 1.1 MPa, closely matching the elastic modulus of native spinal cord tissue, as shown in Figure 6a$_{I}$. Furthermore, its nano-topographical features promoted the adhesion and proliferation of NSCs. More importantly, upon the application of a 500 μA biphasic pulsed ES, the MWCNT conductive network amplified the transduction of electrophysiological signals, thereby activating the differentiation cascade of cells toward neurons and astrocytes, accelerating the growth of nerve cells (Figure 6a$_{II}$). This case study offered a highly promising research direction for CNS repair.

With the evolution of bioelectronic materials, 2D MXene nanosheets have been introduced to the forefront of CNS engineering owing to their exceptional hydrophilicity and high electrical conductivity. Yeh *et al.*[63] developed a novel conductive bioink based on methacryloyl silk fibroin, pectin, and soybean phospholipid-modified MXene, achieving the first direct 3D bioprinting of NSC spheroids (Figure 6b). The incorporation of soybean phospholipid-modified MXene not only endowed the hydrogel with excellent shear-thinning properties and intrinsic electrical conductivity but also moderately reduced its mechanical modulus, providing an ideal soft-matrix mechanical support for neurogenesis. Under a constant daily ES of 300 μA, this conductive network substantially promoted the proliferation and high-ratio neuronal differentiation of NSCs within the printed constructs. It was further validated to potently enhance synaptic vesicle cycling and synaptic transmission activity, thereby achieving a biomimetic reconstruction of the CNS micro-functional network.

Addressing highly complex CNS spinal cord injuries, precisely guiding neural axons to cross the lesion cavity, and reconstructing conduction tracts remain formidable challenges in this field. In 2024, Leahy *et al.*[145] utilized 3D bioprinting technology to precisely construct a PCL framework with pore dimensions highly tailored to the macroscopic anatomical geometry of human corticospinal tracts, and a conductive PPy coating was subsequently deposited onto its surface via *in situ* polymerization (Figure 6c). To further elevate the biomimetic dimension, the research team filled these large conductive microchannels with a neurotrophic ECM rich in collagen IV and fibronectin. When a continuous micro-EF (200 mV/mm) was applied within these highly biomimetic 3D electromechanically coupled channels, neurons whose growth had previously stalled due to the hostile injury microenvironment gained a robust directional driving force for axonal extension, leading to a dramatic increase in the sprouting of long-distance neurites. This bioprinting strategy, combining glial-matrix support with dynamic, targeted electrophysiological stimulation, provides a blueprint for neural bridging following severe spinal cord injuries.

5.2.2. Peripheral nervous system repair

The PNS is an essential conduit connecting the CNS to target organs, maintaining skeletal muscle contraction and sensory activity. Following severe trauma or long-gap defects, despite their intrinsic regenerative capacity, regenerating axons frequently lose spatial directionality. This misdirection induces aberrant axonal coiling and neuroma formation, ultimately causing irreversible denervation-induced fibrosis and target organ atrophy. Consequently, the effective repair of peripheral nerves is of paramount importance for restoring physiological health and overall quality of life.

In neural tissue engineering, biomaterial scaffolds with high electrical conductivity and customized architectures are crucial for facilitating nerve regeneration. PEDOT is a frequently utilized conductive polymer in bioelectronic devices. However, the conventional 3D printing of PEDOT-based conductive scaffolds confronts challenges such as limited printing resolution, poor solubility, and the intrinsic brittleness of the material. Han *et al.*[146] developed a composite ink incorporating PEDOT nanoparticles into GelMA and CS. Utilizing DLP technology, they printed microgrooves that balanced ultra-high resolution with excellent electrical conductivity. *In vitro* experiments coupled with synergistic ES demonstrated that this scaffold promoted axonal elongation in PC12 cells. Furthermore,

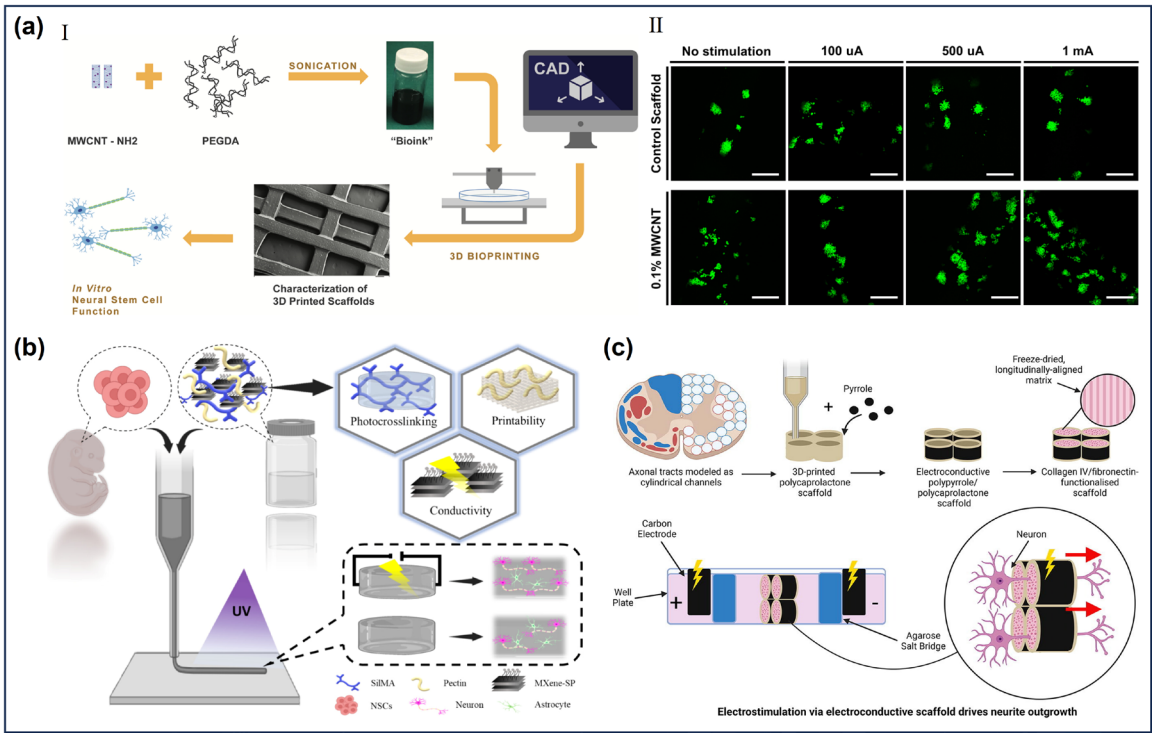

Figure 6. Applications of 3D-printed conductive scaffolds and bioinks synergized with electrical stimulation for central nervous tissue regeneration. (a) 3D-printed nano-conductive scaffolds based on multi-walled carbon nanotubes for nerve regeneration. (I) Schematic illustration of the fabrication process of 3D-printed conductive scaffolds. (II) Schematic diagram of the cell fluorescence comparison under various electrical stimulation parameters. Reprinted with permission from Lee *et al.*[144] Copyright © 2018, IOP Publishing Ltd. (b) Schematic illustration of the innovative MXene/SilMA-based conductive bioink for 3D bioprinting of neural stem cells. Adapted with permission from Yeh *et al.*[63] Copyright © 2025, American Chemical Society. (c) Schematic mechanism of a 3D-printed, biomimetic, neurotrophic, and electroconductive composite scaffold mediating spinal nerve repair via electrostimulation. Adapted with permission from Leahy *et al.*[145] Copyright © 2024, Elsevier Ltd.
Abbreviations: CAD: Computer-aided design; mA: Milliampere; MWCNT-NH_2: Amino-functionalized multi-walled carbon nanotube; MXene-SP: Soybean phospholipid-modified MXene; NH_2: Amino group; NSC: Neural stem cell; PEGDA: Poly(ethylene glycol) diacrylate; SilMA: Silk fibroin methacrylate/glycidyl-methacrylate-modified silk fibroin.

in vivo evaluations demonstrated the successful repair of a 10-mm rat sciatic nerve defect, comprehensively validating the efficacy of the GelMA/CS-PEDOT scaffold in treating peripheral nerve injuries (Figure 7a).

To highly recapitulate the complex composition and micro-electrical properties of the native peripheral nerve ECM, Cheng *et al.*[100] proposed a dual-bioink 3D printing strategy. By combining a conductive GelMA/CS/PPy foundational framework with a degradable gelatin ink loaded with neural cells, they successfully constructed a highly biomimetic double-network conductive scaffold, as illustrated in Figure 7b. Applying exogenous ES (300 mV/cm) within this customized electromechanical microenvironment remarkably upregulated the expression of core genes closely associated with neurogenesis (e.g., *GAP43*, *TUBB3*, *NGFR*, and *NES*). This drove the polarized differentiation of cells toward mature neurons and the formation of synaptic networks, providing a robust translational perspective for peripheral nerve regeneration.

For the *in vivo* application of conductive materials in repairing long-gap defects, the aligned topographical structure and suture-resistant mechanical toughness of the guidance conduit are equally indispensable. In 2020, Zhao *et al.*[147] ingeniously integrated SLA 3D printing with electrospinning technology to precisely fabricate a composite conductive NGC. This NGC featured a PPy/silk fibroin core and a flexible electrospun network shell. Upon seeding with Schwann cells and the application of a 100 mV/mm micro-EF, this conductive framework potently stimulated the paracrine potential of the cells, markedly upregulating the secretion levels of core neurotrophic factors such as brain-derived neurotrophic factor, NT-4/5, and NGF. Evaluated in an *in vivo* 10-mm rat sciatic nerve defect model, this synergistic intervention, combining internally aligned conduction and external flexible wrapping with applied ES, promoted the robust bridging growth of axons and high-quality remyelination (Figure 7c).

Although conventional ES can effectively promote neural regeneration, the use of percutaneous leads poses risks of infection and secondary tissue injury. To overcome this limitation, Fang *et al.*[121] proposed an innovative strategy coupling 4D printing with magnetoelectric conversion. They developed a highly elastic polyurethane-based NGC, precisely exposing porous carbon-based NCs loaded with NGF on its surface, as illustrated in Figure 7d. This smart scaffold responds to non-invasive, high-frequency alternating magnetic fields, generating minuscule eddy currents to deliver direct wireless ES to the cells. More remarkably, the physical alterations triggered by the magnetic field, such as electrostatic repulsion, instantaneously increase the permeability of the nanopores, triggering the on-demand release of the internal NGF. This interventional strategy, which achieves precise spatiotemporal synchronization between a non-invasive physical micro-EF and targeted biochemical factor delivery, substantially increased the myelin sheath thickness of newly formed nerve fibers. It provides a highly promising blueprint for combining wireless ES with bioprinting to facilitate neural repair.

Despite considerable progress, neural tissue engineering still faces several challenges. In CNS repair, precise axonal guidance across lesion sites and functional neural circuit reconstruction remain difficult. Most studies focus on short-term neuronal differentiation rather than long-term functional recovery. In PNS repair, effective regeneration across long-gap defects and prevention of neuroma formation are still major obstacles. In addition, wireless stimulation systems require further improvement in stability, energy efficiency, and biocompatibility. Future research should develop multifunctional scaffolds that integrate topographical, electrical, and biochemical cues. Precise spatiotemporal regulation, combined with real-time monitoring, adaptive stimulation, and biodegradable materials, will be critical for successful clinical translation.

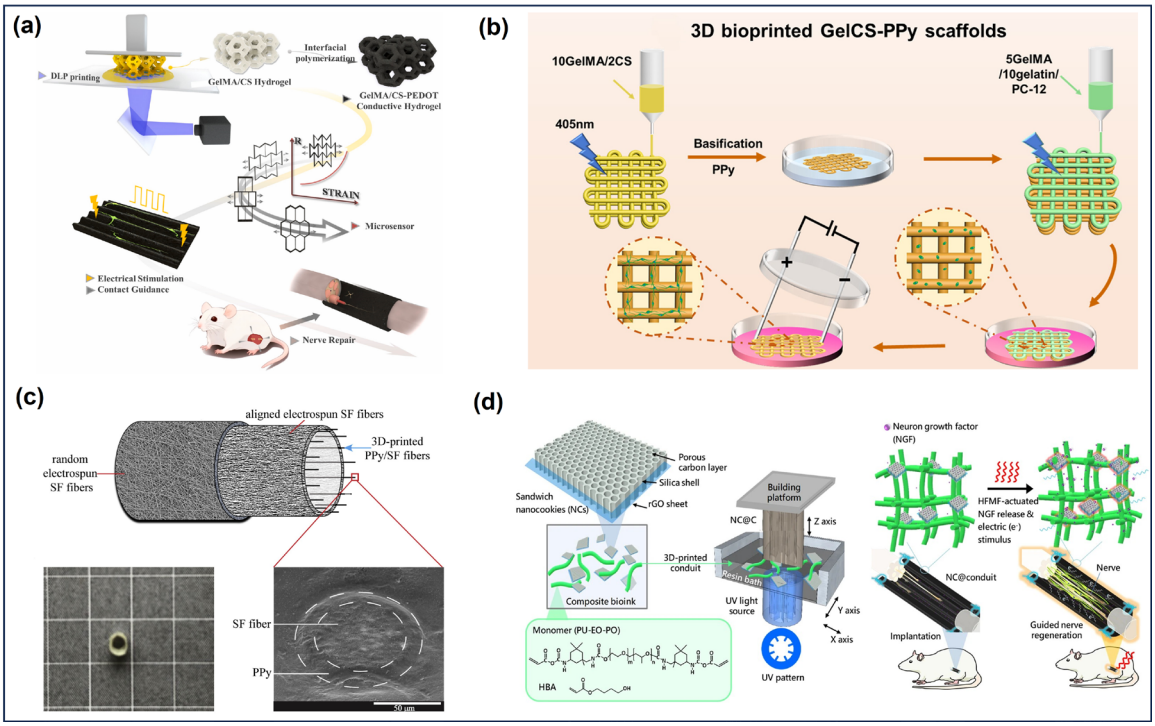

Figure 7. Applications of 3D-printed conductive scaffolds and advanced stimulation strategies in peripheral nervous tissue engineering. (a) Schematic illustration of the fabrication of the GelMA/CS-PEDOT-based bionic double-network conductive scaffold via DLP 3D printing. Reprinted with permission from Han *et al.*[146] Copyright © 2024, Elsevier Ltd. (b) Schematic illustration of the preparation and electrical stimulation of 3D-printed GelCS-PPy conductive scaffolds. Reprinted with permission from Cheng *et al.*[100] Copyright © 2025, Elsevier B.V. (c) Schematic illustration of the structure of the PPy/SF neural scaffold. Reprinted with permission from Zhao *et al.*[147] Copyright © 2020, Elsevier Ltd. (d) Schematic illustration of the 4D-printed stretchable nerve conduit and the mechanism of magnetic-electric stimulation-mediated repair. Adapted with permission from Fang *et al.*[121] Copyright © 2020, Springer Nature.

Abbreviations: CAD: Computer-aided design; CS: Chitosan; DLP: Digital light processing; GelCS: Gelatin/chitosan; GelMA: Gelatin methacryloyl; HBA: 4-Hydroxybutyl acrylate; HFMF: High-frequency magnetic field; NCs: Nanocookies; NGF: Nerve growth factor; PEDOT: Poly(3,4-ethylenedioxythiophene); PPy: Polypyrrole; PU-EO-PO: Urethanepolyethylene glycol-polypropylene glycol monomer; rGO: Reduced graphene oxide; SF: Silk fibroin.

5.3. Bone repair

Bone tissue inherently exhibits piezoelectric properties, generating an endogenous electrical potential that plays an irreplaceable stimulatory role in bone healing. However, in cases of critical-sized bone defects, simple static physical scaffolds frequently suffer from central necrosis due to poor early-stage vascularization and adverse inflammatory responses. In recent years, 3D-printed electroactive scaffolds have provided a revolutionary engineering approach for reconstructing the electrophysiological microenvironment within bone defect regions by integrating conductive networks, *in situ* piezoelectric effects, and exogenous physical interventions.[148-150]

Among early interventional strategies in bone tissue engineering, introducing highly conductive nanomaterials to enhance charge transport efficiency represents a crucial method to accelerate bone repair. In 2021, e Silva *et al.*[151] utilized extrusion-based 3D printing technology to uniformly dope MWCNTs into a PCL matrix, successfully constructing a highly biocompatible composite conductive bone scaffold. In an *in vivo* rat calvarial defect model, the synergistic effect of the MWCNT conductive network and applied ES promoted angiogenesis within the defect region, thereby providing an abundant blood and oxygen supply to support calcium phosphate mineral deposition in the nascent bone matrix. This ultimately induced the formation of thicker, larger-volume, and higher-quality bone tissue (Figure 8a).

Although implantable biomaterials utilizing conductive components to mimic the electrophysiological properties of native tissues have been introduced into the field of bone regeneration, the incorporation of electret materials to deliver stable and sustained ES remains rarely explored. Zhang *et al.*[152] employed melt electrowriting technology to fabricate a ZnO/PCL composite scaffold featuring an *in situ* electret to investigate its efficacy in bone regeneration. Figure 8b illustrates the fabrication process of this scaffold and its underlying mechanisms for promoting bone tissue repair. The micro-EF generated by this scaffold potently suppressed pro-inflammatory M1 macrophages and directed macrophage polarization toward the pro-healing M2 (anti-inflammatory) phenotype. These polarized M2 macrophages secreted high levels of anti-inflammatory cytokines and growth factors. This immune-driven paracrine effect subsequently orchestrated the osteogenic differentiation of BMSCs alongside the tube formation of vascular endothelial cells.

A major challenge in piezoelectric tissue engineering is providing sustained mechanical stimulation to activate piezoelectric scaffolds implanted in deep tissues, such as the femur, where physiological loading is often insufficient. This limitation remains a key barrier to clinical translation. In 2025, Li *et al.*[109] proposed a wireless ES strategy based on low-intensity pulsed ultrasound (LIPUS)-piezoelectric coupling. Utilizing high-resolution DLP 3D bioprinting technology, they covalently encapsulated PEG-modified $BaTiO_3$ piezoelectric nanoparticles and live BMSCs within a GelMA hydrogel framework, achieving integrated cell-laden manufacturing, as shown in Figure 8c. This strategy leverages highly penetrative LIPUS as a non-invasive mechanical force source. When ultrasound waves propagate to the 3D-printed scaffold deep within the body, the generated acoustic stress can *in situ* trigger the polarization of the $BaTiO_3$ nanoparticles, thereby generating ES. In an *in vivo* deep rabbit femoral condyle defect model, this method elevated local bone mineral density and bone volume fraction, achieving high-quality trabecular reconstruction.

Beyond directly inducing intramembranous ossification, cutting-edge electromechanical tissue engineering has begun pivoting toward a repair strategy with higher biomimetic dimensions: endochondral ossification. In a recent study, Ma *et al.*[119] precisely constructed a 3D-printed TENG scaffold based on poly(glycerol sebacate). This scaffold is capable of harvesting subtle biomechanical energy at the implantation site and converting it into an *in situ* pulsed micro-EF. Figure 8d presents a schematic diagram of the scaffold's fabrication and its principles for promoting bone repair. Experimental findings revealed that the triboelectric charges generated by this scaffold could modulate transmembrane calcium ion influx, subsequently profoundly activating the PI3K/Akt signaling pathway and remodeling the actin cytoskeleton. This substantially accelerated the transdifferentiation of chondrocytes into osteoblasts. This method of endochondral ossification offers a novel approach to the repair of bone defects.

In summary, printed electroactive scaffolds are reshaping bone tissue engineering by integrating electrical, mechanical, and biological cues to guide tissue regeneration. Future advances will likely move beyond simple osteogenic stimulation toward precise regulation of bone-immune interactions, vascularized bone formation, and endochondral ossification. The combination of self-powered electrical systems, real-time biosensing, and closed-loop therapeutic regulation may enable dynamic adaptation to different healing stages. Such intelligent and multifunctional platforms hold great promise for the treatment of large and complex bone defects.

5.4. Muscle tissue repair

Muscle is a highly organized and electroactive vital soft tissue. Although skeletal muscle can regenerate following

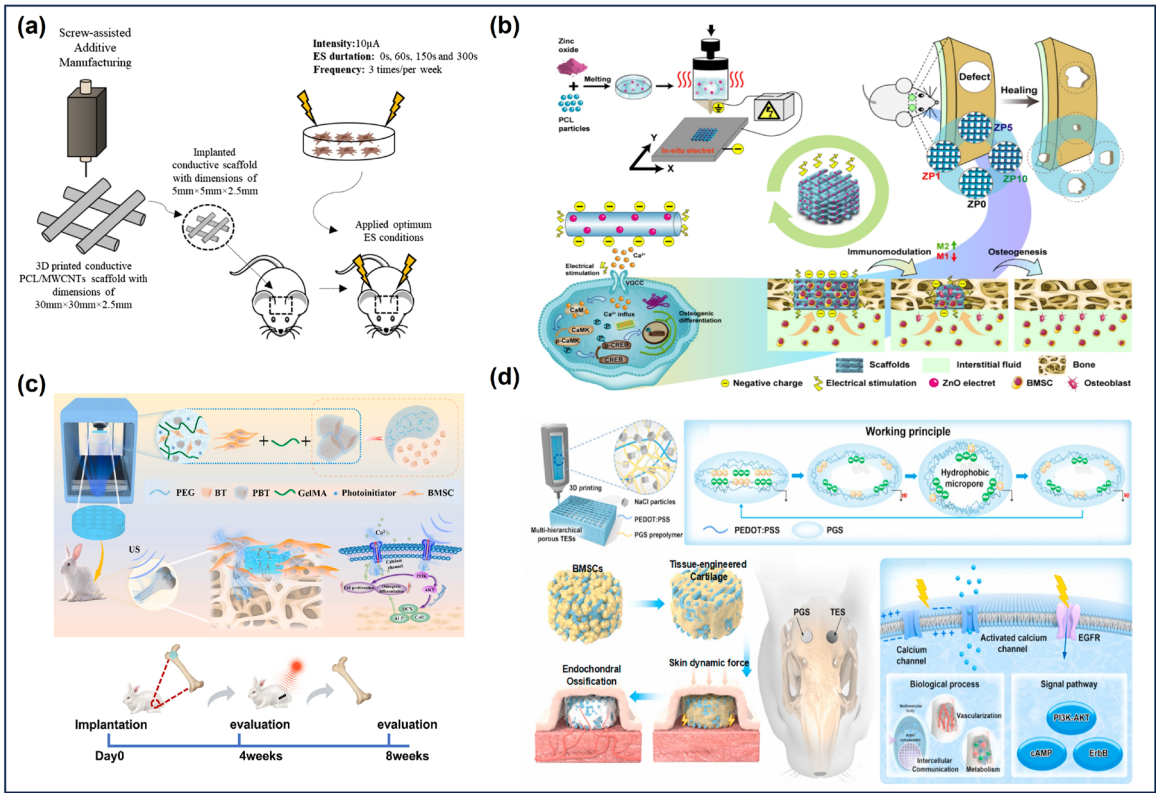

Figure 8. Applications of 3D-printed electroactive scaffolds and diversified electrical stimulation strategies in bone tissue engineering. (a) Schematic illustration of the PCL/MWCNTs-based 3D-printed conductive scaffold combined with exogenous electrical stimulation for bone tissue engineering. Adapted with permission from e Silva *et al.*[151] Copyright © 2021, Springer Nature. (b) Schematic diagram illustrating the preparation of MEW-printed *in situ* electret scaffolds with controllable electric fields and the underlying mechanism for enhancing bone defect regeneration. Reprinted with permission from Zhang *et al.*[152] Copyright © 2024, Elsevier B.V. (c) Schematic diagram illustrating the fabrication process and therapeutic application of 3D-printed Gel/PBT@BMSCs hydrogel scaffolds. Adapted with permission from Li *et al.*[109] Copyright © 2025, Elsevier Ltd. (d) Design of a BMSC-derived cartilage-based TES for bone regeneration and schematic illustration of the mechanism in promoting bone tissue repair. Adapted with permission from Ma *et al.*[119] Copyright © 2026, Elsevier B.V.

Abbreviations: AKT: Protein kinase B; BMSC: Bone marrow mesenchymal stem cell; BT: Barium titanate; cAMP: Cyclic adenosine monophosphate; EGFR: Epidermal growth factor receptor; ErbB: Erythroblastic oncogene B; ES: Electrical stimulation; GelMA: Gelatin methacryloyl; MWCNTs: Multi-walled carbon nanotubes; PBT: PEGylated barium titanate; PCL: Polycaprolactone; PEDOT:PSS: Poly(3,4-ethylenedioxythiophene):poly(styrene sulfonate); PEG: Polyethylene glycol; PGS: Poly(glycerol sebacate); PI3K: Phosphoinositide 3-kinase; TES: Tissue-engineered scaffold; US: Ultrasound; VOCC: Voltage-operated calcium channel; ZP: ZnO/PCL scaffold formulation.

minor injury, its endogenous repair capacity is often inadequate for severe damage such as volumetric muscle loss, leading to fibrosis and irreversible functional deficits. To overcome this limitation, the combination of 3D bioprinting and ES has emerged as a promising approach for muscle regeneration.[153]

In the exploration of constructing an electroactive muscle microenvironment, Wang *et al.*[46] utilized 3D bioprinting technology to develop conductive hydrogel scaffolds capable of enhancing myogenic differentiation. By uniformly integrating conductive PEDOT nanoparticles into GelMA, they not only endowed the bioink with excellent rheological and printability properties but also constructed a continuous conductive network within a 3D space. This 3D-bioprinted conductive scaffold facilitated both intra- and extracellular electrical signal transduction. Various *in vitro* studies have demonstrated the efficacy of the highly conductive GelMA/PEDOT composite scaffold in promoting the proliferation, migration, and differentiation of C2C12 cells (Figure 9a).

The direct incorporation of conductive polymers into hydrogels is frequently hindered by the discontinuity of the resultant conductive networks and the susceptibility of these materials to rapid degradation within physiological fluids. To circumvent this limitation, Fortunato *et al.*[154] proposed a novel fabrication approach utilizing biocompatible gelatin as a flexible load-bearing substrate and a highly conductive PEDOT:PSS solution as a functional ink for

precise deposition via inkjet printing. Experimentally, this device proved capable of delivering exogenous ES to the seeded muscle cells with high fidelity, driving their polar alignment and subsequent differentiation into mature myotubes (Figure 9b).

For volumetric muscle loss, the recapitulation of the parallel-aligned and densely packed myofibrillar architecture inherent in native muscle serves as the physical prerequisite for functional bridging. Bilge *et al.*[155] proposed an innovative strategy that balances structural anisotropy with eco-friendly synthesis: utilizing carbonaceous materials recovered from algal biomass and doping them with MWCNTs to endow the scaffold with excellent electrical conductivity. Leveraging 3D printing technology, this conductive ink was precisely patterned into scaffolds with a parallel-aligned topology, as depicted in Figure 9c. This biomimetic design faithfully recapitulated the native muscle microenvironment. While providing electrophysiological signals, it regulated the polar extension of myocytes via physical contact guidance, demonstrating tremendous potential for muscle regeneration.

Beyond static conductive networks, dynamic bioelectrical cues driven by physiological mechanical forces offer a more biomimetically significant solution for skeletal muscle tissue engineering. In 2025, Sonaye *et al.*[156] developed a novel bioink possessing piezoelectric properties using natural bioactive materials such as SA, gelatin, and CS. Employing extrusion-based 3D bioprinting technology, they constructed a high-resolution composite scaffold with a mechanical modulus closely matching the stiffness of native muscle (Figure 9d). Crucially, when subjected to external mechanical forces, the scaffold's

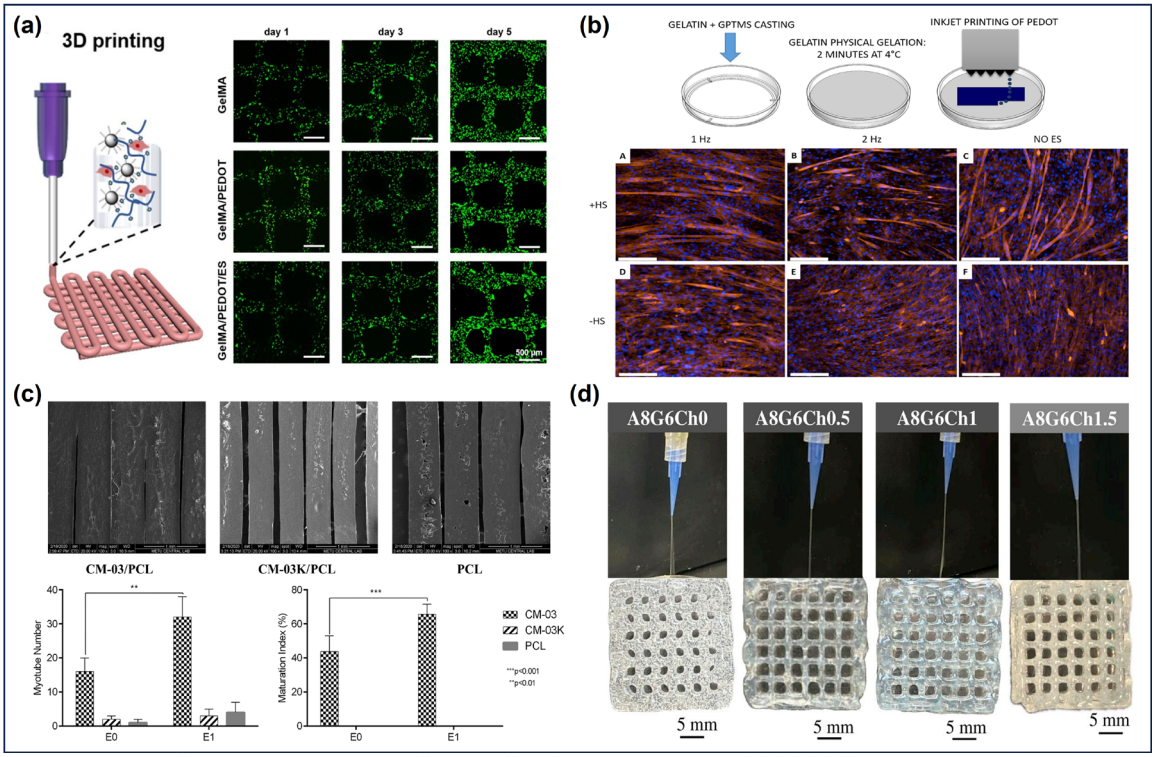

Figure 9. Applications of 3D-printed electroactive scaffolds and advanced manufacturing technologies in muscle tissue engineering. (a) Schematic illustration of the fabrication of 3D-bioprinted conductive hydrogel scaffolds for enhanced myogenic differentiation (left). Live (green)/dead (red) staining of C2C12 cells in the GelMA/PEDOT hydrogel scaffolds after 1, 3, and 5 days (right). Adapted with permission from Wang *et al.*[46] Copyright © 2021, Oxford University Press. (b) Schematic illustration of inkjet printing of PEDOT on a cross-linked gelatin substrate (top). Comparison of DAPI (nuclei) and Phalloidin TRITC (cytoplasm) staining under 1 Hz, 2 Hz, and no electrical stimulation after 7 days (bottom). Reprinted with permission from Fortunato *et al.*[154] Copyright © 2018, Elsevier B.V. (c) Schematic diagrams of different 3D-printed scaffold structures (top). Comparison of the number of myotubes and maturity index calculated from MHC staining (bottom). Adapted with permission from Bilge *et al.*[155] Copyright © 2021, Springer Nature. (d) Schematic diagram of printed scaffold structures using different bioink formulations. Reprinted with permission from Sonaye *et al.*[156] Copyright © 2025, Sage Publications.

Abbreviations: Ch: Chitosan; CM: Carbonaceous material; G: Gelatin; GelMA: Gelatin methacryloyl; GPTMS: 3-Glycidyloxypropyltrimethoxysilane; HS: Horse serum; PCL: Polycaprolactone/poly(ε-caprolactone); PEDOT: Poly(3,4-ethylenedioxythiophene); PEDOT:PSS: Poly(3,4-ethylenedioxythiophene) :poly(styrene sulfonate).

piezoelectric properties can *in situ* generate localized ES. The synergistic effect of this electromechanical conversion mechanism and excellent biocompatibility promoted the adhesion and differentiation of C2C12 muscle cells, providing an active regenerative therapeutic strategy for treating severe soft tissue trauma.

Overall, electroactive scaffolds have shown great promise for enhancing myogenesis and promoting functional muscle regeneration. However, muscle repair still struggles with recapitulating aligned myofibrillar architecture and preventing fibrosis after volumetric loss. Future research should move beyond enhancing myogenic differentiation toward the coordinated reconstruction of muscle fibers, vascular networks, and neuromuscular junctions. In addition, mechanoresponsive and self-powered bioelectronic materials may provide biomimetic stimulation that better matches the physiological demands of regenerating muscle. Such advanced multifunctional platforms are expected to improve muscle strength, contractile performance, and tissue integration.

5.5. Cardiac tissue repair

Ischemic myocardial injury, such as myocardial infarction, leads to irreversible cardiomyocyte death and the formation of electrically insulating fibrotic scar tissue, which disrupts normal cardiac electrical conduction and synchronized contractile function, potentially resulting in cardiogenic shock and death. Given the limited regenerative capacity of cardiomyocytes, conventional static scaffolds are insufficient to restore the damaged electrophysiological microenvironment. In recent years, the integration of 3D printing technology with ES has emerged as a highly promising bioengineering strategy for reconstructing cardiac electrical conduction networks, modulating cellular electrophysiology, and restoring contractile function.

In the early exploration of cardiac tissue engineering, researchers attempted to exploit ES to investigate the role of EFs in promoting the *in vitro* maturation of cardiomyocytes. In 2017, Adams *et al.*[157] employed 3D printing to fabricate 3D cell culture scaffolds with controlled pore architectures using PCL and silicone rubber as substrate materials. A multichannel external ES system capable of wireless control via smartphone was developed, wherein graphite rod electrodes positioned within culture wells delivered localized pulsed EFs to the insulating scaffolds. Results demonstrated that PCL scaffolds exhibited superior cytocompatibility; furthermore, under external ES at 5 V and 1 Hz, primary human cardiomyocytes seeded on these scaffolds displayed markedly elevated cell density, with a substantial proportion of cells exhibiting prominent cytoplasmic actin pseudopodial extensions, thereby confirming the constructive role of EF intervention in promoting cardiomyocyte structural differentiation (Figure 10a).

Despite the efficacy achieved through external ES, ideal cardiac repair materials should possess intrinsic electrical conductivity and recapitulate the highly organized anisotropic architecture of native myocardium. To this end, Ul Haq *et al.*[158] employed 3D micro-SLA to precisely fabricate conductive scaffolds mimicking the hierarchically aligned lamellar organization of myocardial muscle fibers, as illustrated in Figure 10b. The photocurable conductive bioink consisted of a ternary composite of photosensitive PEGDA, the conductive polymer PANI, and curcumin serving as a light-absorbing photoinitiator dye. The incorporation of curcumin functioned as a liquid optical filter, effectively regulating light penetration depth and ensuring high-fidelity resolution during 3D fabrication. The resulting biomimetic scaffold not only exhibited a well-defined microstructured architecture but also demonstrated favorable semiconducting properties, supporting ionic diffusion and electron transfer between the polymer matrix and the surrounding electrolytic medium, thereby providing cardiomyocytes with a conducive biomimetic conductive interface.

To translate such *in vitro* conductive scaffolds toward *in vivo* orthotopic therapeutic applications, the development of implantable conductive cardiac patches with high flexibility and tissue compliance has become a critical objective. In 2024, Luque *et al.*[159] designed a printable conductive cardiac patch based on PEDOT for myocardial tissue remodeling, as depicted in **Figure 10c**. The hydrogel matrix, composed of PVA, PEDOT, and gallic acid as a supramolecular dynamic crosslinking agent, demonstrated exceptional elasticity, mechanical robustness, and thermoreversible phase transition characteristics, rendering it well-suited for direct-write 3D printing via melt extrusion. In adult murine models, the patch efficiently conducted electrical pacing signals with ultralow impedance to trigger intracellular calcium transients without inducing any malignant arrhythmias following epicardial implantation. Crucially, magnetic resonance imaging monitoring revealed that the patch provided both mechanical support and electrical conduction pathways to the infarcted myocardium, significantly improving left ventricular ejection fraction and stroke volume.

The aforementioned approaches frequently rely on lead implantation or conductive networks to transmit external pacing signals, which may cause secondary physical injury or foreign body responses. To fundamentally overcome these limitations, Ershad *et al.*[126] proposed a passive, wireless cross-scale heterogeneous integration strategy in

2025, as shown in Figure 10d. Solid-state microscale solar cells (μ-solar cells) fabricated via micro/nanofabrication processes were physically dispersed as discrete microfillers within GelMA hydrogel, constructing a novel class of photoelectroactive bioink. Through extrusion-based 3D printing, this bioink was co-cultured with cardiomyocytes to form 3D cardiac constructs with light-responsive electrophysiological characteristics. Upon illumination at specific wavelengths, the embedded μ-solar cells instantaneously converted photonic energy into localized microcurrents *in situ*. This ES mechanism, based on the physical integration of devices, has successfully enabled the wireless and on-demand pacing of cardiac tissue beating rhythms, opening up highly futuristic application prospects for next-generation smart cardiac patches and fully non-invasive bioelectronic devices.

The synergistic strategy combining 3D printing and ES has achieved notable progress in repairing tissues such as skin, nerve, bone, and myocardium, and shows broad therapeutic potential. With next-generation high-precision printing technologies and intelligent bioinks on the horizon, this approach is expected to overcome current interdisciplinary challenges and extend its applications to more complex pathological scenarios.

6. Conclusion and future perspectives

Although combining 3D bioprinting with ES shows great promise for repairing complex tissue defects, several technical challenges must be addressed before clinical use. First, the precise molecular pathways by which ES governs tissue repair need to be further elucidated. Different tissues respond differently to different electrical characteristics

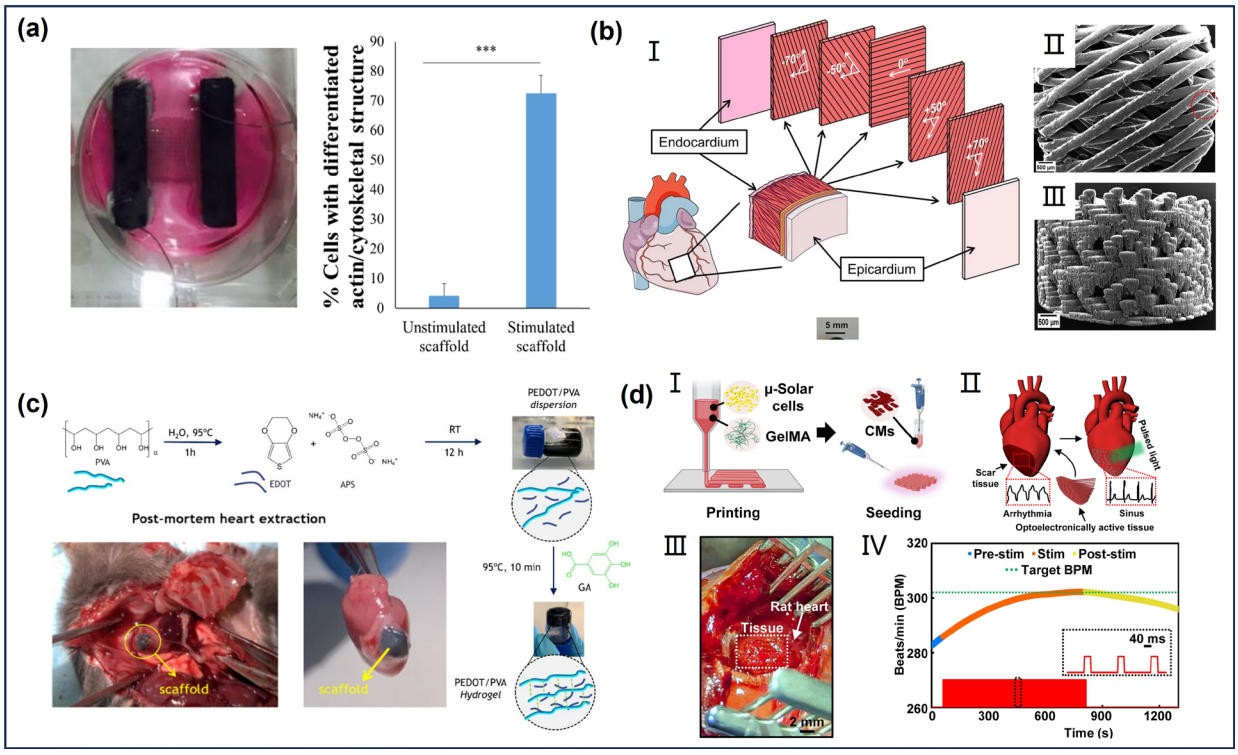

Figure 10. Applications of 3D-printed electroactive scaffolds and diversified electrical stimulation strategies in cardiac tissue engineering. (a) Schematic illustration of electrical stimulation of primary human cardiomyocytes on a PCL-based scaffold (left). A graph showing the percentage of cells with differentiated actin structure in both stimulated and unstimulated tests (right). Reprinted with permission from Adams *et al.*[157] Copyright © 2017, Elsevier B.V. (b) Schematic diagram of the myofibrils in myocardium and printed scaffolds. (I) The myofibers are oriented at different angles in a hierarchical manner. (II & III) Scanning electron microscopy images of the printed scaffold. Adapted with permission from Ul Haq *et al.*[158] Copyright © 2023, Springer Nature. (c) Schematic diagram of the PVA-GA/PEDOT hydrogel preparation process and the conductive scaffold applied to the heart. Reprinted with permission from Luque *et al.*[159] Copyright © 2024, American Chemical Society. (d) Schematic diagram of a 3D-printed optoelectronic scaffold for cardiac pacing. (I) Schematic diagram of a 3D-printed optoelectronic scaffold. (II) Example of *in vivo* implantation of a printed optoelectronically active tissue and correction of arrhythmic beating. (III) Schematic diagram of the optoelectronically active tissue on the rat heart surface. (IV) Beating rate of rat hearts following optoelectronic stimulation. Adapted with permission from Ershad *et al.*[126] Copyright © 2025, AAAS.
Abbreviations: APS: Ammonium persulfate; BPM: Beats per minute; CMs: Cardiomyocytes; EDOT: 3,4-Ethylenedioxythiophene; GA: Gallic acid; GelMA: Gelatin methacryloyl; PEDOT: Poly(3,4-ethylenedioxythiophene); PVA: Poly(vinyl alcohol); RT: Room temperature; stim: Stimulation.

such as frequency, intensity, and waveform. Further studies are needed to clarify the underlying mechanisms by which cells transduce external electrical inputs into intracellular responses via membrane receptors.[40] Second, current 3D printing technologies face difficulties in balancing high-resolution hierarchical structures with mechanical strength. Particularly challenging is the fabrication of large scaffolds with uniformly distributed conductive networks, as uneven current distribution can readily damage cells.[56] Third, an ideal scaffold must not only maintain stable electrical activity during the regeneration process but also be capable of eventual degradation in the body. However, conventional conductive polymers such as PEDOT:PSS and PPy lack intrinsic biodegradability and are prone to charge decay in physiological environments. Therefore, developing novel electroactive materials that can degrade safely without compromising a stable conductive network remains a significant challenge.[83,160]

Looking forward, ongoing research will help fully clarify the molecular mechanisms by which ES promotes tissue repair. Driven by rapid advances in integrated circuits and bioelectronics, future ES systems will become highly miniaturized and intelligent, enabling adaptive, high-precision modulation of electrical signals tailored to different tissues and regenerative stages.[161] In biofabrication, further developments in 3D bioprinting will enable the precise creation of native micro- and nano-architectures, including dense capillary networks, which ensure a seamless integration of the printed scaffold with the host tissue.[162] In materials science, future conductive bioinks will not require a bulky external power source. Scaffolds may be engineered as self-powered micro-generators through the incorporation of piezoelectric, triboelectric, magnetoelectric, bio-battery, or optoelectronic nanomaterials that harvest mechanical, magnetic, biochemical, or light energy.[163,164] In addition, advanced bioinks are also expected to achieve temporal programmability, enabling controlled modulus changes or on-demand release of growth factors at specific healing stages, potentially aided by 4D printing strategies and artificial intelligence-guided formulation design.[165] Finally, developing fully biodegradable electroactive materials that safely degrade in sync with new tissue formation remains the critical step toward clinical success.[166]

In summary, the paradigm of integrating 3D-printed conductive scaffolds with ES has shifted from passive physical support to active electrophysiological guidance. The combination of materials science, biofabrication, and bioelectronics will soon enable this area to progress beyond the simple bridging of tissues toward the construction of fully functional smart tissues. Through the precise spatiotemporal control of both electrical signals and material properties, we are on the verge of realizing the functional restoration of complex organs, thereby opening a new chapter in regenerative medicine.

Acknowledgments

None.

Funding

This work was supported by the National Natural Science Foundation of China (NSFC, no. 62304264) and the Basic and Applied Basic Research Foundation of Guangdong Province (no. 2025A1515010752, 2026A1515011564).

Conflict of interest

The authors declare no conflicts of interest.

Author contributions

Conceptualization: Huachun Wang
Visualization: Jiaming Wu, Jinglin Ye, Lihu Chen, Wenxiao Fang
Writing–original draft: Jinwei Huang, Huachun Wang
Writing–review & editing: Jinwei Huang, Huachun Wang

Ethics approval and consent to participate

Not applicable.

Consent for publication

Not applicable.

Availability of data

Not applicable.

References

1. Nunes CO, Barriga EH. Bioelectricity in Morphogenesis. *Annu Rev Cell Dev Biol.* 2025;41:187-208.

   doi: 10.1146/annurev-cellbio-101323-032747

2. Zhang G, Levin M, Kozminski K. Bioelectricity Is a Universal Multifaced Signaling Cue in Living Organisms. *Mol Biol Cell.* 2025;36(2):pe2.

   doi: 10.1091/mbc.E23-08-0312

3. Ferreira F, Moreira S, Zhao M, Barriga EH. Stretch-Induced Endogenous Electric Fields Drive Directed Collective Cell Migration in Vivo. *Nat Mater.* 2025;24(3):462-470.

   doi: 10.1038/s41563-024-02060-2

4. Zhao M. Electrical Fields in Wound Healing—An Overriding Signal That Directs Cell Migration. *Semin Cell Dev Biol.* 2009;20(6):674-682.

   doi: 10.1016/j.semcdb.2008.12.009

5. Balint R, Cassidy NJ, Cartmell SH. Electrical Stimulation: A Novel Tool for Tissue Engineering. *Tissue Eng Part B Rev.* 2013;19(1):48-57.

   doi: 10.1089/ten.teb.2012.0183

6. Huang Y, Yao K, Zhang Q, *et al*. Bioelectronics for Electrical Stimulation: Materials, Devices and Biomedical Applications. *Chem Soc Rev.* 2024;53(17):8632-8712.

   doi: 10.1039/D4CS00413B

7. Zhang K, De Maria D, Jebakumar M, *et al*. The Bionic Interface: Considering the Material Mediated Electrical Stimulation of Stem Cells. *Adv Mater.* 2026;38(2):e12399.

   doi: 10.1002/adma.202512399

8. Deng K, Luo R, Chen Y, *et al*. Electrical Stimulation Therapy – Dedicated to the Perfect Plastic Repair. *Adv Sci.* 2025;12(24):2409884.

   doi: 10.1002/advs.202409884

9. Sundaramurthi D, Rauf S, Hauser CAE. 3D Bioprinting Technology for Regenerative Medicine Applications. *Int J Bioprinting.* 2016;2(2):9-26.

   doi: 10.18063/IJB.2016.02.010

10. Tripathi S, Mandal SS, Bauri S, Maiti P. 3D Bioprinting and Its Innovative Approach for Biomedical Applications. *MedComm.* 2023;4(1):e194.

    doi: 10.1002/mco2.194

11. Kazemi M, Maralbashi S. Advances in 3D Bioprinting for Medical Application: Opportunities and Challenges. *BioMed Eng OnLine.* 2025;25(1):11.

    doi: 10.1186/s12938-025-01498-y

12. Asim S, Tabish TA, Liaqat U, Ozbolat IT, Rizwan M. Advances in Gelatin Bioinks to Optimize Bioprinted Cell Functions. *Adv Healthc Mater.* 2023;12(17):2203148.

    doi: 10.1002/adhm.202203148

13. S S, R G AP, Bajaj G, *et al*. A Review on the Recent Applications of Synthetic Biopolymers in 3D Printing for Biomedical Applications. *J Mater Sci Mater Med.* 2023;34(12):62.

    doi: 10.1007/s10856-023-06765-9

14. Wang X, Ao Q, Tian X, *et al*. Gelatin-Based Hydrogels for Organ 3D Bioprinting. *Polymers.* 2017;9(9):401.

    doi: 10.3390/polym9090401

15. Rai R, Roether JA, Boccaccini AR. Polyaniline Based Polymers in Tissue Engineering Applications: A Review. *Prog Biomed Eng.* 2022;4(4):042004.

    doi: 10.1088/2516-1091/ac93d3

16. Tran CM, Yue Z, Qin C, *et al*. 3D Printing of Conducting Polymer Hydrogels for Electrostimulation-Assisted Tissue Engineering. *Adv Mater.* 2025;37(36):2507779.

    doi: 10.1002/adma.202507779

17. Byrne R, Redmond J, Rochfort KD, *et al*. A Thermoresponsive, Electrically Conductive Bioink Optimized for Electroactive Tissue Engineering and Bioelectronics. *ACS Appl Bio Mater.* 2026;9(6):2895-2913.

    doi: 10.1021/acsabm.5c02097

18. Vijayavenkataraman S, Vialli N, Fuh JYH, Lu WF. Conductive Collagen/Polypyrrole-b-Polycaprolactone Hydrogel for Bioprinting of Neural Tissue Constructs. *Int J Bioprinting.* 2019;5(2.1):229.

    doi: 10.18063/ijb.v5i2.1.229

19. Olate-Moya F, Fernández-Gil F, Solano L, Córdova L, Palza H. Multifunctional Electroactive 3D-Printed Scaffolds with Polypyrrole-Based Coatings for Biomedical Applications. *Macromol Rapid Commun.* 2025;46(23):e00246.

    doi: 10.1002/marc.202500246

20. Li S, Shan Y, Chen J, *et al*. 3D Printing and Biomedical Applications of Piezoelectric Composites: A Critical Review. *Adv Mater Technol.* 2025;10(5):2401160.

    doi: 10.1002/admt.202401160

21. Rahul TP, Sreekanth PSR. Synergies in Materials and Manufacturing: A Review of Composites and 3D Printing for Triboelectric Energy Harvesting. *J Compos Sci.* 2025;9(8):386.

    doi: 10.3390/jcs9080386

22. Wibowo A, Vyas C, Cooper G, *et al*. 3D Printing of Polycaprolactone–Polyaniline Electroactive Scaffolds for Bone Tissue Engineering. *Materials.* 2020;13(3):512.

    doi: 10.3390/ma13030512

23. Katoh K. Effects of Electrical Stimulation of the Cell: Wound Healing, Cell Proliferation, Apoptosis, and Signal Transduction. *Med Sci.* 2023;11(1):11.

    doi: 10.3390/medsci11010011

24. Chen C, Bai X, Ding Y, Lee I-S. Electrical Stimulation as a Novel Tool for Regulating Cell Behavior in Tissue Engineering. *Biomater Res.* 2019;23(1):25.

    doi: 10.1186/s40824-019-0176-8

25. Babona-Pilipos R, Droujinine IA, Popovic MR, Morshead CM. Adult Subependymal Neural Precursors, but Not Differentiated Cells, Undergo Rapid Cathodal Migration in the Presence of Direct Current Electric Fields. *PLoS One.* 2011;6(8):e23808.

    doi: 10.1371/journal.pone.0023808

26. Meng X, Arocena M, Penninger J, *et al*. PI3K Mediated Electrotaxis of Embryonic and Adult Neural Progenitor Cells in the Presence of Growth Factors. *Exp Neurol.* 2011;227(1):210-217.

    doi: 10.1016/j.expneurol.2010.11.002

27. Bai H, Forrester JV, Zhao M. DC Electric Stimulation Upregulates Angiogenic Factors in Endothelial Cells through Activation of VEGF Receptors. *Cytokine.* 2011;55(1):110-115.

doi: 10.1016/j.cyto.2011.03.003

28. Babona-Pilipos R, Liu N, Pritchard-Oh A, *et al*. Calcium Influx Differentially Regulates Migration Velocity and Directedness in Response to Electric Field Application. *Exp Cell Res.* 2018;368(2):202-214.

doi: 10.1016/j.yexcr.2018.04.031

29. Liu Q, Song B. Electric Field Regulated Signaling Pathways. *Int J Biochem Cell Biol.* 2014;55:264-268.

doi: 10.1016/j.biocel.2014.09.014

30. Kavaliauskaitė J, Kazlauskaitė A, Lazutka JR, Mozolevskis G, Stirkė A. Pulsed Electric Fields Alter Expression of NF-κB Promoter-Controlled Gene. *Int J Mol Sci.* 2021;23(1):451.

doi: 10.3390/ijms23010451

31. Zhang Z, Wu C, Yang J, *et al*. Hypoxic Preconditioning Promotes Galvanotaxis of Human Dermal Microvascular Endothelial Cells through NF-κB Pathway. *Heliyon.* 2022;8(12):12421.

doi: 10.1016/j.heliyon.2022.e12421

32. Yu J, Ramirez LM, Lin Q, Burz DS, Shekhtman A. Ribosome External Electric Field Regulates Metabolic Enzyme Activity: The RAMBO Effect. *J Phys Chem B.* 2024;128(29):7002-7021.

doi: 10.1021/acs.jpcb.4c00628

33. Thrivikraman G, Boda SK, Basu B. Unraveling the Mechanistic Effects of Electric Field Stimulation towards Directing Stem Cell Fate and Function: A Tissue Engineering Perspective. *Biomaterials.* 2018;150:60-86.

doi: 10.1016/j.biomaterials.2017.10.003

34. Bahar E, Kim H, Yoon H. ER Stress-Mediated Signaling: Action Potential and Ca2+ as Key Players. *Int J Mol Sci.* 2016;17(9):1558.

doi: 10.3390/ijms17091558

35. Sempou E, Kostiuk V, Zhu J, *et al*. Membrane Potential Drives the Exit from Pluripotency and Cell Fate Commitment via Calcium and mTOR. *Nat Commun.* 2022;13(1):6681.

doi: 10.1038/s41467-022-34363-w

36. Wang Y, Cui H, Wu Z, *et al*. Modulation of Osteogenesis in MC3T3-E1 Cells by Different Frequency Electrical Stimulation. *PLoS One.* 2016;11(5):e0154924.

doi: 10.1371/journal.pone.0154924

37. Love MR, Palee S, Chattipakorn SC, Chattipakorn N. Effects of Electrical Stimulation on Cell Proliferation and Apoptosis. *J Cell Physiol.* 2018;233(3):1860-1876.

doi: 10.1002/jcp.25975

38. Estlack LE, Roth CC, Thompson GL, Lambert WA, Ibey BL. Nanosecond Pulsed Electric Fields Modulate the Expression of Fas/CD95 Death Receptor Pathway Regulators in U937 and Jurkat Cells. *Apoptosis.* 2014;19(12):1755-1768.

doi: 10.1007/s10495-014-1041-9

39. Gu J, He X, Chen X, *et al*. Effects of Electrical Stimulation on Cytokine-Induced Macrophage Polarization. *J Tissue Eng Regen Med.* 2022;16(5):448-459.

doi: 10.1002/term.3292

40. Preetam S, Ghosh A, Mishra R, *et al*. Electrical Stimulation: A Novel Therapeutic Strategy to Heal Biological Wounds. *RSC Adv.* 2024;14(44):32142-32173.

doi: 10.1039/D4RA04258A

41. Rae CD, Lee VH-C, Ordidge RJ, Alonzo A, Loo C. Anodal Transcranial Direct Current Stimulation Increases Brain Intracellular pH and Modulates Bioenergetics. *Int J Neuropsychopharmacol.* 2013;16(8):1695-1706.

doi: 10.1017/S1461145713000084

42. Stalder D, Gershlick DC. Direct Trafficking Pathways from the Golgi Apparatus to the Plasma Membrane. *Semin Cell Dev Biol.* 2020;107:112-125.

doi: 10.1016/j.semcdb.2020.04.001

43. Geng K, Wang J, Liu P, *et al*. Electrical Stimulation Facilitates the Angiogenesis of Human Umbilical Vein Endothelial Cells through MAPK/ERK Signaling Pathway by Stimulating FGF2 Secretion. *Am J Physiol Cell Physiol.* 2019;317(2):C277-C286.

doi: 10.1152/ajpcell.00474.2018

44. Bean AC, Sahu A, Piechocki C, *et al*. Neuromuscular Electrical Stimulation Enhances the Ability of Serum Extracellular Vesicles to Regenerate Aged Skeletal Muscle after Injury. *Exp Gerontol.* 2023;177:112179.

doi: 10.1016/j.exger.2023.112179

45. Murphy SV, Atala A. 3D Bioprinting of Tissues and Organs. *Nat Biotechnol.* 2014;32(8):773-785.

doi: 10.1038/nbt.2958

46. Wang Y, Wang Q, Luo S, *et al*. 3D Bioprinting of Conductive Hydrogel for Enhanced Myogenic Differentiation. *Regen Biomater.* 2021;8(5):rbab035.

doi: 10.1093/rb/rbab035

47. Vu M, Pramanik A, Basak AK, Prakash C, Shankar S. Progress and Challenges on Extrusion Based Three Dimensional (3D) Printing of Biomaterials. *Bioprinting.* 2022;27:e00223.

doi: 10.1016/j.bprint.2022.e00223

48. Ng WL, An J, Chua CK. Process, Material, and Regulatory Considerations for 3D Printed Medical Devices and Tissue Constructs. *Engineering.* 2024;36:146-166.

doi: 10.1016/j.eng.2024.01.028

49. Carou-Senra P, Rodríguez-Pombo L, Awad A, *et al*. Inkjet Printing of Pharmaceuticals. *Adv Mater.* 2024;36(11):2309164.

    doi: 10.1002/adma.202309164

50. Tao H, Zhang X, Yuan X, *et al*. 3D Bioprinting Technology in Tissue Engineering Printing Method and Material Selection. *BioNanoSci.* 2025;15(1):199.

    doi: 10.1007/s12668-025-01816-7

51. Martinelli A, Nitti A, Po R, Pasini D. 3D Printing of Layered Structures of Metal-Ionic Polymers: Recent Progress, Challenges and Opportunities. *Materials.* 2023;16(15):5327.

    doi: 10.3390/ma16155327

52. Azizi Machekposhti S, Mohaved S, Narayan RJ. Inkjet Dispensing Technologies: Recent Advances for Novel Drug Discovery. *Expert Opin Drug Discov.* 2019;14(2):101-113.

    doi: 10.1080/17460441.2019.1567489

53. Wallace ER, Yue Z, Dottori M, *et al*. Point of Care Approaches to 3D Bioprinting for Wound Healing Applications. *Prog Biomed Eng.* 2023;5(2):023002.

    doi: 10.1088/2516-1091/acceeb

54. Duocastella M, Fernández-Pradas JM, Morenza JL, Zafra D, Serra P. Novel Laser Printing Technique for Miniaturized Biosensors Preparation. *Sens Actuators B Chem.* 2010;145(1):596-600.

    doi: 10.1016/j.snb.2009.11.055

55. Kingsley DM, Roberge CL, Rudkouskaya A, *et al*. Laser-Based 3D Bioprinting for Spatial and Size Control of Tumor Spheroids and Embryoid Bodies. *Acta Biomater.* 2019;95:357-370.

    doi: 10.1016/j.actbio.2019.02.014

56. Zandrini T, Florczak S, Levato R, Ovsianikov A. Breaking the Resolution Limits of 3D Bioprinting: Future Opportunities and Present Challenges. *Trends Biotechnol.* 2023;41(5):604-614.

    doi: 10.1016/j.tibtech.2022.10.009

57. Sekar MP, Subramanian A, Sundaramurthi D, Sethuraman S. Srishti: A Custom-Built Laser-Assisted 3D Bioprinter for Fabricating High-Resolution Biological Constructs. *BMC Methods.* 2026;3(1):2.

    doi: 10.1186/s44330-025-00051-6

58. Li Y, Zhang X, Zhang X, Zhang Y, Hou D. Recent Progress of the Vat Photopolymerization Technique in Tissue Engineering: A Brief Review of Mechanisms, Methods, Materials, and Applications. *Polymers.* 2023;15(19):3940.

    doi: 10.3390/polym15193940

59. Ng WL, Paula CTB, Serra AC, Coelho JFJ, Bartolo P. Vat Photopolymerization-Based Bioprinting: Shaping next-Generation Tissues with Light. *Interdiscip Med.* 2026;4(1):e70078.

    doi: 10.1002/inmd.70078

60. Li W, Wang M, Ma H, *et al*. Stereolithography Apparatus and Digital Light Processing-Based 3D Bioprinting for Tissue Fabrication. *iScience.* 2023;26(2):106039.

    doi: 10.1016/j.isci.2023.106039

61. Santoni S, Gugliandolo SG, Sponchioni M, Moscatelli D, Colosimo BM. 3D Bioprinting: Current Status and Trends—a Guide to the Literature and Industrial Practice. *Bio-Des Manuf.* 2022;5(1):14-42.

    doi: 10.1007/s42242-021-00165-0

62. Geng Q, Wang D, Chen P, Chen S-C. Ultrafast Multi-Focus 3-D Nano-Fabrication Based on Two-Photon Polymerization. *Nat Commun.* 2019;10(1):2179.

    doi: 10.1038/s41467-019-10249-2

63. Yeh Y-C, Chen P-Y, Chen K-T, Lee I-C. Innovative MXene/SilMA-Based Conductive Bioink for Three Dimensional Bioprinting of Neural Stem Cell Spheroids in Neural Tissue Engineering. *ACS Appl Mater Interfaces.* 2025;17(7):10402-10416.

    doi: 10.1021/acsami.4c19373

64. He Z, He S. Two-Photon Polymerization of Hydrogel Cellular Scaffolds. *Opt Commun.* 2025;574:131161.

    doi: 10.1016/j.optcom.2024.131161

65. Yang Y, Xu X, Wang B, *et al*. Optimisation of Curing Models and Ultra-High-Precision Forming Strategy in Vat Photopolymerization of Silica-Based Ceramic Modified by Graphene. *Virtual Phys Prototyp.* 2025;20(1):e2499450.

    doi: 10.1080/17452759.2025.2499450

66. Bukhari SMZS, Bukhari MA, Hossain M. Vat Photopolymerization of Smart Polymers for Biomedical Applications. *ACS Appl Polym Mater.* 2025;7(18):12117-12144.

    doi: 10.1021/acsapm.5c01487

67. Sun J, Gong Y, He Y, *et al*. Process Optimization for Coaxial Extrusion-Based Bioprinting: A Comprehensive Analysis of Material Behavior, Structural Precision, and Cell Viability. *Addit Manuf.* 2025;100:104682.

    doi: 10.1016/j.addma.2025.104682

68. Liu W, Zhong Z, Hu N, *et al*. Coaxial Extrusion Bioprinting of 3D Microfibrous Constructs with Cell-Favorable Gelatin Methacryloyl Microenvironments. *Biofabrication.* 2018;10(2):024102.

    doi: 10.1088/1758-5090/aa9d44

69. Davoodi E, Sarikhani E, Montazerian H, *et al*. Extrusion and Microfluidic-Based Bioprinting to Fabricate Biomimetic Tissues and Organs. *Adv Mater Technol.* 2020;5(8):1901044.

    doi: 10.1002/admt.201901044

70. Mei X, Yang Z, Wang X, *et al*. Integrating Microfluidic and Bioprinting Technologies: Advanced Strategies for Tissue Vascularization. *Lab Chip.* 2025;25(5):764-786.

doi: 10.1039/D4LC00280F

71. Ravanbakhsh H, Luo Z, Zhang X, *et al*. Freeform Cell-Laden Cryobioprinting for Shelf-Ready Tissue Fabrication and Storage. *Matter.* 2022;5(2):573-593.

doi: 10.1016/j.matt.2021.11.020

72. Luo Z, Tang G, Ravanbakhsh H, *et al*. Vertical Extrusion Cryo(Bio)Printing for Anisotropic Tissue Manufacturing. *Adv Mater.* 2022;34(12):2108931.

doi: 10.1002/adma.202108931

73. Weygant J, Entezari A, Koch F, *et al*. Droplet 3D Cryobioprinting for Fabrication of Free-Standing and Volumetric Structures. *Aggregate.* 2024;5(5):e599.

doi: 10.1002/agt2.599

74. Chang J, He J, Lei Q, Li D. Electrohydrodynamic Printing of Microscale PEDOT:PSS-PEO Features with Tunable Conductive/Thermal Properties. *ACS Appl Mater Interfaces.* 2018;10(22):19116-19122.

doi: 10.1021/acsami.8b04051

75. Kang H-W, Lee SJ, Ko IK, *et al*. A 3D Bioprinting System to Produce Human-Scale Tissue Constructs with Structural Integrity. *Nat Biotechnol.* 2016;34(3):312-319.

doi: 10.1038/nbt.3413

76. Schwab A, Levato R, D'Este M, *et al*. Printability and Shape Fidelity of Bioinks in 3D Bioprinting. *Chem Rev.* 2020;120(19):11028-11055.

doi: 10.1021/acs.chemrev.0c00084

77. Ma X, Xu M, Cui X, Yin J, Wu Q. Hybrid 3D Bioprinting of Sustainable Biomaterials for Advanced Multiscale Tissue Engineering. *Small.* 2026;22(16):2408947.

doi: 10.1002/smll.202408947

78. Li Z, Chen L, Wu J, *et al*. A Review of 3D Bioprinting for Organoids. *Med Rev.* 2025;5(4):318-338.

doi: 10.1515/mr-2024-0089

79. Garciamendez-Mijares CE, Ruiz DSR, Kuang X, *et al*. Acoustic Bioprinting: A Glimpse Into an Emerging Field. *Small Methods.* 2026;10(3):2500733.

doi: 10.1002/smtd.202500733

80. Gungor-Ozkerim PS, Inci I, Zhang YS, Khademhosseini A, Dokmeci MR. Bioinks for 3D Bioprinting: An Overview. *Biomater Sci.* 2018;6(5):915-946.

doi: 10.1039/C7BM00765E

81. Raja JKB, Díaz GY, Boucan FSOL, *et al*. Advances in Decellularized Extracellular Matrix Bioinks for Regenerative Medicine Applications. *Int J Bioprinting.* 2025;11(5):23-45.

doi: 10.36922/IJB025210205

82. Athukorala SS, Tran TS, Balu R, *et al*. 3D Printable Electrically Conductive Hydrogel Scaffolds for Biomedical Applications: A Review. *Polymers.* 2021;13(3):474.

doi: 10.3390/polym13030474

83. Distler T, Boccaccini AR. 3D Printing of Electrically Conductive Hydrogels for Tissue Engineering and Biosensors – A Review. *Acta Biomater.* 2020;101:1-13.

doi: 10.1016/j.actbio.2019.08.044

84. Wu Y, Ganguly S, Tang XS. 3D Bioprinting of Anisotropic Filler-Reinforced Polymer Nanocomposites: Synthesis, Assembly, and Multifunctional Applications. *Int J Bioprinting.* 2024;10(2):1637.

doi: 10.36922/ijb.1637

85. Yuk H, Lu B, Lin S, *et al*. 3D Printing of Conducting Polymers. *Nat Commun.* 2020;11(1):1604.

doi: 10.1038/s41467-020-15316-7

86. Zhang S, Chen Y, Liu H, *et al*. Room-Temperature-Formed PEDOT:PSS Hydrogels Enable Injectable, Soft, and Healable Organic Bioelectronics. *Adv Mater.* 2020;32(1):1904752.

doi: 10.1002/adma.201904752

87. Menzel VC, Yi X, Bößl F, *et al*. Additive Manufacturing of Polyaniline Electrodes for Electrochemical Applications. *Addit Manuf.* 2022;54:102710.

doi: 10.1016/j.addma.2022.102710

88. Zea M, Texidó R, Villa R, Borrós S, Gabriel G. Specially Designed Polyaniline/Polypyrrole Ink for a Fully Printed Highly Sensitive pH Microsensor. *ACS Appl Mater Interfaces.* 2021;13(28):33524-33535.

doi: 10.1021/acsami.1c08043

89. Ahn J, Sim HH, Kim JH, *et al*. Air-Pressure-Assisted Pen-Nib Printing for 3D Printed Electronics. *Adv Mater Technol.* 2022;7(6):2101172.

doi: 10.1002/admt.202101172

90. Yang J, Cao Q, Tang X, *et al*. 3D-Printed Highly Stretchable Conducting Polymer Electrodes for Flexible Supercapacitors. *J Mater Chem A.* 2021;9(35):19649-19658.

doi: 10.1039/D1TA02617H

91. Liu J, Mckeon L, Garcia J, *et al*. Additive Manufacturing of Ti3C2-MXene-Functionalized Conductive Polymer Hydrogels for Electromagnetic-Interference Shielding. *Adv Mater.* 2022;34(5):2106253.

doi: 10.1002/adma.202106253

92. Ghaffarkhah A, Kamkar M, Dijvejin ZA, *et al*. High-Resolution Extrusion Printing of Ti3C2-Based Inks for Wearable Human Motion Monitoring and Electromagnetic Interference Shielding. *Carbon.* 2022;191:277-289.

doi: 10.1016/j.carbon.2022.02.003

93. He Y, Li J, Zhang L, *et al*. 3D-Printed GA/PPy Aerogel Biocathode Enables Efficient Methane Production in Microbial Electrosynthesis. *Chem Eng J.* 2023;459:141523.

doi: 10.1016/j.cej.2023.141523

94. Meng J, Zhou T, Tai W, *et al*. Self-Assembled MXene/Polyaniline Gels Enable 3D-Printed Micro-Supercapacitors with High Energy Storage. *ACS Appl Energy Mater.* 2026;9(4):2387-2397.

doi: 10.1021/acsaem.5c04016

95. Spencer AR, Shirzaei Sani E, Soucy JR, *et al*. Bioprinting of a Cell-Laden Conductive Hydrogel Composite. *ACS Appl Mater Interfaces.* 2019;11(34):30518-30533.

doi: 10.1021/acsami.9b07353

96. Buzio M, Gini M, Schneider TC, *et al*. 3D Micropatterning of PEDOT:PSS/Gelatin Conductive Hydrogels via Two-Photon Lithography for Soft Bioelectronics. *npj Flex Electron.* 2026;10(1):19.

doi: 10.1038/s41528-026-00529-5

97. Scordo G, Bertana V, Ballesio A, *et al*. Effect of Volatile Organic Compounds Adsorption on 3D-Printed PEGDA:PEDOT for Long-Term Monitoring Devices. *Nanomaterials.* 2021;11(1):94.

doi: 10.3390/nano11010094

98. Zhang X, Li D, Liu G. 3D Printed Ultrasoft and Adhesive PEDOT:PSS-Based Hydrogel for Bioelectronics. *ACS Appl Polym Mater.* 2025;7(3):1531-1539.

doi: 10.1021/acsapm.4c03275

99. Wan R, Liu S, Li Z, *et al*. 3D Printing of Highly Conductive and Strongly Adhesive PEDOT:PSS Hydrogel-Based Bioelectronic Interface for Accurate Electromyography Monitoring. *J Colloid Interface Sci.* 2025;677:198-207.

doi: 10.1016/j.jcis.2024.05.171

100. Cheng R, Liu Z, Li M, *et al*. Peripheral Nerve Regeneration with 3D Printed Bionic Double-Network Conductive Scaffold Based on GelMA/Chitosan/Polypyrrole. *Int J Biol Macromol.* 2025;304:140746.

doi: 10.1016/j.ijbiomac.2025.140746

101. Ma C, Jiang L, Wang Y, *et al*. 3D Printing of Conductive Tissue Engineering Scaffolds Containing Polypyrrole Nanoparticles with Different Morphologies and Concentrations. *Materials.* 2019;12(15):2491.

doi: 10.3390/ma12152491

102. Serafin A, Culebras M, Oliveira JM, Koffler J, Collins MN. 3D Printable Electroconductive Gelatin-Hyaluronic Acid Materials Containing Polypyrrole Nanoparticles for Electroactive Tissue Engineering. *Adv Compos Hybrid Mater.* 2023;6(3):109.

doi: 10.1007/s42114-023-00665-w

103. Bao X, Meng J, Tan Z, *et al*. Direct-Ink-Write 3D Printing of Highly-Stretchable Polyaniline Gel with Hierarchical Conducting Network for Customized Wearable Strain Sensors. *Chem Eng J.* 2024;491:151918.

doi: 10.1016/j.cej.2024.151918

104. Carcione R, Roppolo I, Chiappone A, *et al*. Role of Precursors and Doping Agents in Producing 3D-Printed PEGDA–PDANI Electroactive Composites by an In Situ Polymerization Approach. *ACS Appl Polym Mater.* 2024;6(2):1159-1168.

doi: 10.1021/acsapm.3c02086

105. Xu M, Wei C, Zhang Y, *et al*. Coplanar Conformational Structure of π-Conjugated Polymers for Optoelectronic Applications. *Adv Mater.* 2024;36(1):2301671.

doi: 10.1002/adma.202301671

106. Li J, Cao J, Lu B, Gu G. 3D-Printed PEDOT:PSS for Soft Robotics. *Nat Rev Mater.* 2023;8(9):604-622.

doi: 10.1038/s41578-023-00587-5

107. Liang J, Zeng H, Qiao L, *et al*. 3D Printed Piezoelectric Wound Dressing with Dual Piezoelectric Response Models for Scar-Prevention Wound Healing. *ACS Appl Mater Interfaces.* 2022;14(27):30507-30522.

doi: 10.1021/acsami.2c04168

108. Li B, Ma Y, Fatima K, *et al*. 3D Printed Shape-Memory Piezoelectric Scaffolds with in-Situ Self-Power Properties for Bone Defect Repair. *J Nanobiotechnol.* 2025;23(1):244.

doi: 10.1186/s12951-025-03325-x

109. Li M, Hu X, Liu X, *et al*. 3D Bioprinted Piezoelectric Hydrogel Synergized with LIPUS to Promote Bone Regeneration. *Mater Today Bio.* 2025;31:101604.

doi: 10.1016/j.mtbio.2025.101604

110. Sikder P, Nagaraju P, Naganaboyina HPS. 3D-Printed Piezoelectric Porous Bioactive Scaffolds and Clinical Ultrasonic Stimulation Can Help in Enhanced Bone Regeneration. *Bioengineering.* 2022;9(11):679.

doi: 10.3390/bioengineering9110679

111. Polley C, Distler T, Detsch R, *et al*. 3D Printing of Piezoelectric Barium Titanate-Hydroxyapatite Scaffolds with Interconnected Porosity for Bone Tissue Engineering. *Materials.* 2020;13(7):1773.

doi: 10.3390/ma13071773

112. Chen P, Xu C, Wu P, *et al*. Wirelessly Powered Electrical-Stimulation Based on Biodegradable 3D Piezoelectric Scaffolds Promotes the Spinal Cord Injury Repair. *ACS Nano.* 2022;16(10):16513-16528.

doi: 10.1021/acsnano.2c05818

113. Huang X, Liang J, Jia Q, *et al*. A 3D-Printed

Piezoelectric Scaffold With Bio-Inspired Gradient and Dynamic Adaptation for Tendon Regeneration. *Adv Mater.* 2026;38(15):e17298.

doi: 10.1002/adma.202517298

114. Meena KK, Arief I, Nag A, Nagel J, Das A. 3D-Printed PVDF-Based Hybrid Nanogenerators With Dominant Triboelectric Output for High-Sensitivity Force Sensing. *IEEE Sens J.* 2025;25(14):26412-26420.

doi: 10.1109/JSEN.2025.3572337

115. Zain Karimy NH, Li H, Lee HB, *et al*. Highly Efficient 3D-Printed PVDF-Based Triboelectric Nanogenerators Featuring Polymorphic Perovskite Nanofillers. *Adv Funct Mater.* 2025;35(39):2424271.

doi: 10.1002/adfm.202424271

116. Zhuo L, Zeng J, Chen Q, *et al*. 3D-Printed Hygroscopic Polymer Networks for High-Humidity Triboelectric Nanogenerators to Wirelessly Power Implantable Electronic Devices- A Conceptual Pathway. *Adv Funct Mater.* 2026;36(46):e75354.

doi: 10.1002/adfm.75354

117. Jurinovs M, Lapčinskis L, Sherrell PC, Gaidukovs S, Šutka A. Printing Bioderived and Biodegradable Triboelectric Nanogenerators via Dual-Head Additive Manufacturing. *ACS Sustainable Chem Eng.* 2025;13(12):4641-4650.

doi: 10.1021/acssuschemeng.4c06702

118. Yi Q, Pei X, Das P, *et al*. A Self-Powered Triboelectric MXene-Based 3D-Printed Wearable Physiological Biosignal Sensing System for on-Demand, Wireless, and Real-Time Health Monitoring. *Nano Energy.* 2022;101:107511.

doi: 10.1016/j.nanoen.2022.107511

119. Ma Y, Song X, Luo B, *et al*. 3D-Printed Triboelectric Scaffolds for Fabricating BMSC-Derived Cartilage to Repair Bone Defects and Promote Endochondral Ossification. *Bioact Mater.* 2026;58:685-700.

doi: 10.1016/j.bioactmat.2025.11.044

120. Kaviani Y, Eslami H, Ansari M, Poursamar SA. 3D Printed Magnetoactive Nanocomposite Scaffolds for Bone Regeneration. *Biomed Mater.* 2024;20(1):015028.

doi: 10.1088/1748-605X/ad9f04

121. Fang J-H, Hsu H-H, Hsu R-S, *et al*. 4D Printing of Stretchable Nanocookie@conduit Material Hosting Biocues and Magnetoelectric Stimulation for Neurite Sprouting. *NPG Asia Mater.* 2020;12(1):61.

doi: 10.1038/s41427-020-00244-1

122. Dong M, Wang X, Chen X-Z, *et al*. 3D-Printed Soft Magnetoelectric Microswimmers for Delivery and Differentiation of Neuron-Like Cells. *Adv Funct Mater.* 2020;30(17):1910323.

doi: 10.1002/adfm.201910323

123. Liu L, Gao Y, Lee S, Choi S. 3D Bioprinting of Cyanobacteria for Solar-Driven Bioelectricity Generation in Resource-Limited Environments. In: *2018 40th Annual International Conference of the IEEE Engineering in Medicine and Biology Society (EMBC)*. Piscataway, NJ: IEEE; 2018:5329-5332.

doi: 10.1109/EMBC.2018.8513490

124. Wang X, Han F, Xiao Z, *et al*. 3-D Printable Living Hydrogels as Portable Bio-Energy Devices. *Adv Mater.* 2025;37(18):2419249.

doi: 10.1002/adma.202419249

125. Reyes C, Fivaz E, Sajó Z, *et al*. 3D Printed Cellulose-Based Fungal Battery. *ACS Sustainable Chem Eng.* 2024;12(43):16001-16011.

doi: 10.1021/acssuschemeng.4c05494

126. Ershad F, Rao Z, Maharajan S, *et al*. Bioprinted Optoelectronically Active Cardiac Tissues. *Sci Adv.* 2025;11(4):eadt7210.

doi: 10.1126/sciadv.adt7210

127. Luo B, Zhou Q, Chen W, *et al*. Nonadjacent Wireless Electrotherapy for Tissue Repair by a 3D-Printed Bioresorbable Fully Soft Triboelectric Nanogenerator. *Nano Lett.* 2023;23(7):2927-2937.

doi: 10.1021/acs.nanolett.3c00300

128. Luo R, Dai J, Zhang J, Li Z. Accelerated Skin Wound Healing by Electrical Stimulation. *Adv Healthc Mater.* 2021;10(16):2100557.

doi: 10.1002/adhm.202100557

129. Tyler SEB. Nature's Electric Potential: A Systematic Review of the Role of Bioelectricity in Wound Healing and Regenerative Processes in Animals, Humans, and Plants. *Front Physiol.* 2017;8:627.

doi: 10.3389/fphys.2017.00627

130. Burgess JL, Wyant WA, Abujamra BA, Kirsner RS, Jozic I. Diabetic Wound-Healing Science. *Medicina.* 2021;57(10):1072.

doi: 10.3390/medicina57101072

131. Yin M, Wang Y, Wei Y, *et al*. 3D-Printed Hydrogels for Treating Diabetic Wounds: Recent Developments. *Int J Bioprinting.* 2025;11(6):107-129.

doi: 10.36922/IJB025320322

132. Wang AYL, Aviña AE, Liu Y-Y, Kao H-K. Skin Bioprinting for Burn Reconstruction: From Stem Cell Integration to Smart in Situ Regenerative Systems. *Int J Bioprinting.* 2025;11(6):130-196.

doi: 10.36922/IJB025360364

133. Kumi M, Hou Z, Zhang Y, *et al*. 3D Printed Chitosan-Based Flexible Electrode with Antimicrobial Properties for

Electrical Stimulation Therapy in Wound Healing. *Supramol Mater.* 2025;4:100110.

doi: 10.1016/j.supmat.2025.100110

134. Lee J-J, Ng HY, Lin Y-H, *et al*. The 3D Printed Conductive Grooved Topography Hydrogel Combined with Electrical Stimulation for Synergistically Enhancing Wound Healing of Dermal Fibroblast Cells. *Biomater Adv.* 2022;142:213132.

doi: 10.1016/j.bioadv.2022.213132

135. Nie N, Gong L, Jiang D, *et al*. 3D Bio-Printed Endometrial Construct Restores the Full-Thickness Morphology and Fertility of Injured Uterine Endometrium. *Acta Biomater.* 2023;157:187-199.

doi: 10.1016/j.actbio.2022.12.016

136. Zhou Q, Dai H, Yan Y, *et al*. From Short Circuit to Completed Circuit: Conductive Hydrogel Facilitating Oral Wound Healing. *Adv Healthc Mater.* 2024;13(15):2303143.

doi: 10.1002/adhm.202303143

137. Ling Z, Zhang H, Zhao J, *et al*. Electrostimulation-Based Decellularized Matrix Bladder Patch Promotes Bladder Repair in Rats. *ACS Biomater Sci Eng.* 2024;10(10):6498-6508.

doi: 10.1021/acsbiomaterials.4c00961

138. Gao Z, Pang Z, Chen Y, *et al*. Restoring After Central Nervous System Injuries: Neural Mechanisms and Translational Applications of Motor Recovery. *Neurosci Bull.* 2022;38(12):1569-1587.

doi: 10.1007/s12264-022-00959-x

139. Gu D, Xia Y, Ding Z, *et al*. Inflammation in the Peripheral Nervous System after Injury. *Biomedicines.* 2024;12(6):1256.

doi: 10.3390/biomedicines12061256

140. Ye J, Huang J, Nie W, *et al*. Implantable Nongenetic Optoelectronic Biointerfaces for Neuromodulation. *Adv Photonics Res.* 2025;6(12):e202500176.

doi: 10.1002/adpr.202500176

141. Wu L, Gao H, Han Q, *et al*. Piezoelectric Materials for Neuroregeneration: A Review. *Biomater Sci.* 2023;11(22):7296-7310.

doi: 10.1039/D3BM01111A

142. Li J, Wu C, Zeng M, *et al*. Functional Material-Mediated Wireless Physical Stimulation for Neuro-Modulation and Regeneration. *J Mater Chem B.* 2023;11(38):9056-9083.

doi: 10.1039/D3TB01354E

143. Zhang Y, Chen S, Xiao Z, *et al*. Magnetoelectric Nanoparticles Incorporated Biomimetic Matrix for Wireless Electrical Stimulation and Nerve Regeneration. *Adv Healthc Mater.* 2021;10(16):2100695.

doi: 10.1002/adhm.202100695

144. Lee S-J, Zhu W, Nowicki M, *et al*. 3D Printing Nano Conductive Multi-Walled Carbon Nanotube Scaffolds for Nerve Regeneration. *J Neural Eng.* 2018;15(1):016018.

doi: 10.1088/1741-2552/aa95a5

145. Leahy LM, Woods I, Gutierrez-Gonzalez J, *et al*. Electrostimulation via a 3D-Printed, Biomimetic, Neurotrophic, Electroconductive Scaffold for the Promotion of Axonal Regrowth after Spinal Cord Injury. *Mater Today.* 2024;79:60-72.

doi: 10.1016/j.mattod.2024.07.015

146. Han Y, Sun M, Lu X, *et al*. A 3D Printable Gelatin Methacryloyl/Chitosan Hydrogel Assembled with Conductive PEDOT for Neural Tissue Engineering. *Compos Part B Eng.* 2024;273:111241.

doi: 10.1016/j.compositesb.2024.111241

147. Zhao Y, Liang Y, Ding S, *et al*. Application of Conductive PPy/SF Composite Scaffold and Electrical Stimulation for Neural Tissue Engineering. *Biomaterials.* 2020;255:120164.

doi: 10.1016/j.biomaterials.2020.120164

148. Wang L, Liu Y, Fan Z. Techniques, Mechanisms, and Application of 3D-Printed Biodegradable Metals for Bone Regeneration. *Int J Bioprinting.* 2024;10(3):2460.

doi: 10.36922/ijb.2460

149. Wu L, Zhao J, Huang J, Huang P, Zhao H. Advances and Challenges in Three-Dimensional Bioprinting of Bone Organoids: Materials, Techniques, and Functionalization Strategies. *Int J Bioprinting.* 2025;11(5):1-22.

doi: 10.36922/IJB025190183

150. Yang J, Wang J, Yang Y, *et al*. 3D-Printed Bioactive Scaffolds: An Emerging Strategy for the Regeneration of Infectious Bone Defects. *Int J Bioprinting.* 2024;11(2):79-138.

doi: 10.36922/ijb.4986

151. e Silva EP, Huang B, Helaehil JV, *et al*. In Vivo Study of Conductive 3D Printed PCL/MWCNTs Scaffolds with Electrical Stimulation for Bone Tissue Engineering. *Bio-Des Manuf.* 2021;4(2):190-202.

doi: 10.1007/s42242-020-00116-1

152. Zhang X, Qiao Z, Lian M, *et al*. In-Situ Electret Scaffolds with Controllable Electric Fields Printed by MEW for Bone Tissue Regeneration. *Chem Eng J.* 2024;496:154330.

doi: 10.1016/j.cej.2024.154330

153. Liu X, Xu M, Wang H, Zhu L. Bioprinting Strategies for Skeletal Muscle Regeneration: Advances in Bioinks, Technologies, and Functional Reconstruction. *Int J Bioprinting.* 2025;11(5):46-67.

doi: 10.36922/IJB025300306

154. Fortunato GM, De Maria C, Eglin D, Serra T, Vozzi G. An Ink-Jet Printed Electrical Stimulation Platform for Muscle

Tissue Regeneration. *Bioprinting.* 2018;11:e00035.

doi: 10.1016/j.bprint.2018.e00035

155. Bilge S, Ergene E, Talak E, *et al.* Recycled Algae-Based Carbon Materials as Electroconductive 3D Printed Skeletal Muscle Tissue Engineering Scaffolds. *J Mater Sci Mater Med.* 2021;32(7):73.

doi: 10.1007/s10856-021-06534-6

156. Sonaye SY, Bohara S, Welsh BL, *et al.* Extrusion-Based 3D Bioprinting of Bioactive and Piezoelectric Scaffolds as Potential Therapy for Treating Critical Soft Tissue Wounds. *Adv Wound Care.* 2025;14(3):143-158.

doi: 10.1089/wound.2024.0073

157. Adams SD, Ashok A, Kanwar RK, Kanwar JR, Kouzani AZ. Integrated 3D Printed Scaffolds and Electrical Stimulation for Enhancing Primary Human Cardiomyocyte Cultures. *Bioprinting.* 2017;6:18-24.

doi: 10.1016/j.bprint.2017.04.003

158. Ul Haq A, Montaina L, Pescosolido F, *et al.* Electrically Conductive Scaffolds Mimicking the Hierarchical Structure of Cardiac Myofibers. *Sci Rep.* 2023;13(1):2863.

doi: 10.1038/s41598-023-29780-w

159. Luque GC, Picchio ML, Daou B, *et al.* Printable Poly(3,4-Ethylenedioxythiophene)-Based Conductive Patches for Cardiac Tissue Remodeling. *ACS Appl Mater Interfaces.* 2024;16(27):34467-34479.

doi: 10.1021/acsami.4c03784

160. Kenry, Liu B. Recent Advances in Biodegradable Conducting Polymers and Their Biomedical Applications. *Biomacromolecules.* 2018;19(6):1783-1803.

doi: 10.1021/acs.biomac.8b00275

161. Leng Y, Sun R. Multifunctional Biomedical Devices with Closed-Loop Systems for Precision Therapy. *Adv Healthc Mater.* 2025;14(31):2500860.

doi: 10.1002/adhm.202500860

162. Kim MS, Choi Y, Lee KY. Three-Dimensional Printing and Bioprinting Strategies for Cardiovascular Constructs: From Printing Inks to Vascularization. *Polymers.* 2025;17(17):2337.

doi: 10.3390/polym17172337

163. Razack RK, Sadasivuni KK. Advancing Nanogenerators: The Role of 3D-Printed Nanocomposites in Energy Harvesting. *Polymers.* 2025;17(10):1367.

doi: 10.3390/polym17101367

164. Ahmed A, Azam A, Wang Y, *et al.* Additively Manufactured Nano-Mechanical Energy Harvesting Systems: Advancements, Potential Applications, Challenges and Future Perspectives. *Nano Converg.* 2021;8(1):37.

doi: 10.1186/s40580-021-00289-0

165. Abolhassani S, Fattahi R, Safshekan F, Saremi J, Hasanzadeh E. Advances in 4D Bioprinting: The Next Frontier in Regenerative Medicine and Tissue Engineering Applications. *Adv Healthc Mater.* 2025;14(4):2403065.

doi: 10.1002/adhm.202403065

166. Sojdeh S, Panjipour A, Castillo M, Arabpour Z, Djalilian AR. Emerging Smart and Adaptive Hydrogels for Next-Generation Tissue Engineering. *Bioengineering.* 2025;13(1):50.

doi: 10.3390/bioengineering13010050